# Peptide-functionalized Polymeric Nanoparticles for Cancer Therapy Applications

**Sílvia Catarina da Silva Lobo**

Thesis to obtain the Master of Science Degree in

**Microbiology**

Supervisors: Dr. Nuno Filipe Santos Bernardes

Dr. Karina Marangoni

## Examination Committee

Chairperson: Prof. Jorge Humberto Gomes Leitão

Supervisors: Dr. Nuno Filipe Santos Bernardes

Members of Committee: Dr. Sandra Cristina Nunes Trigo Fernandes Pinto

**October 2022**

# PREFACE

The work presented in this thesis was performed at the Institute for Bioengineering and Bioscience of Instituto Superior Técnico (Lisbon, Portugal), during the period November 2021-July 2022, under the supervision of Dr. Nuno Bernardes and Dr. Karina Marangoni within the frame of the *Fundação para a Ciência e a Tecnologia* (FCT) funded project “p28Nano - Cell penetrating p28 peptide mediated delivery of nanomedicines for cancer treatment” (PTDC/BTM-SAL/30034/2017).

# DECLARATION

I declare that this document is an original work of my own authorship and that it fulfils all the requirements of the Code of Conduct and Good Practices of the *Universidade de Lisboa*.

# ACKNOWLEDGEMENTS

First and foremost, I would like to express my gratitude to Professor Arsénio Fialho, for allowing me to participate in this research project and for his help and knowledge throughout my master's thesis.

I would like to express my sincere gratitude to my supervisor Doctor Nuno Bernardes for the continuous support on my work, for his patience, availability, and immense knowledge. He guided me even before being my supervisor and always gave me the help I needed, especially in the time of research, in the laboratory, and writing this thesis, and for all that I am grateful.

I also thank Doctor Karina Marangoni for helping me in the beginning of my journey, for teaching me all her techniques and laboratory tips, and finally, for always being cheerful and in a good mood, which lessened the pain of sometimes having to be at Técnico before 8am.

I would like to thank the Institute for Bioengineering and Biosciences (iBB) and *Fundação para a Ciência e a Tecnologia* (FCT) for the financial support. The funding by FCT to the scientific project p28 Nano Cell penetrating p28 peptide mediated delivery of nanomedicines for cancer treatment (PTDC/BTM-SAL/30034/2017).

I would like to thank my friends for all the support in the most complicated moments and I believe that with them, and all the coffee breaks we took, made all of this work easier and less stressful.

I would also like to thank my parents for their support, for always being there for me, and especially for their interest and curiosity in whatever I do, even though they pretend to understand it. And lastly, but definitely not least, a special thanks to my brother who always gives me strength and I know that if he was here, he would be very proud of me.

# ABSTRACT

Azurin is a copper-containing redox protein secreted by the bacterium *Pseudomonas aeruginosa* composed by 128 amino acids (aa). This protein can enter cancer cells and induce apoptosis, thereby causing cytotoxic effects in tumor tissues. A small fragment of the protein containing 28 amino acid residues, usually called the p28 peptide, is the protein domain associated, at least in part, to the protein's antiproliferative activity in cancer cells. This peptide has extensively been studied as a possible cancer therapy, alone or in combination with other therapies. Our group has recently studied the functionalization of polymeric nanoparticles (NPs) made of PLGA, with or without the encapsulation of chemotherapeutic drugs to demonstrate its elevated ability to promote the activity of anticancer drugs in lung cancer cells. It has been demonstrated that the peptide's N-terminal domain can be associated with its preferential entry while its C-terminal can be more associated to the anticancer activity. Therefore, the first objective of this thesis, was to functionalize polymeric nanoparticles with the N-terminal region of p28 containing the first 18 amino acid residues (p18 peptide), to understand the interaction of p18-functionalized NPs with A549 lung cancer cells. For the second objective, a new experiment with PLGA-p28-NPs was made to study their effect at the level of plasma membrane organization of A549 cells, when these were incubated with functionalized NPs (250 μg/mL), non-functionalized NPs (250 μg/mL), free p28 (2.5 μM), and free p28 (50 μM). The evaluation was possible with the use of the fluorescent probe Laurdan and a two-photon excitation microscopy.

For the experiment with p18, the cell-NP interaction of p18 functionalized and non-functionalized NPs was performed in A549 lung cancer cells and 16HBE14o- human bronchial non-cancer cells through flow cytometry. These results were compared with those obtained by previous studies of p28 to see if this new fragment of 18 aa brings any advantage in terms of cell interaction, and it was concluded that p18 does not promote a stronger interaction with cells than p28, therefore it does not bring more advantages than p28. In the second objective of this thesis, every condition appears to interfere with the fluidity of the plasma membrane when compared to the control. Our preliminary data evidence that Free p28 (2.5 μM) was the treatment that caused the most membrane perturbation, reinforcing that p28 may lead to a decrease content of lipid rafts, which confers a higher membrane order and stability of cancer cells.

## KEYWORDS

Nanoparticles | p18 | p28 | Cancer | Laurdan

# RESUMO

A azurina é uma proteína redox de cobre secretada pela bactéria *Pseudomonas aeruginosa* composta por 128 aminoácidos (aa). Esta proteína pode entrar nas células cancerígenas e induzir apoptose, causando assim efeitos citotóxicos nos tecidos tumorais. Um pequeno fragmento da proteína contendo 28 resíduos de aminoácidos, normalmente chamado péptido p28, é o domínio proteico associado, pelo menos em parte, à atividade antiproliferativa da proteína nas células cancerígenas. Este péptido tem sido estudado extensivamente como uma possível terapia do cancro, sozinho ou em combinação com outras terapias. O nosso grupo estudou recentemente a funcionalização de nanopartículas (NPs) poliméricas formuladas com PLGA, com ou sem o encapsulamento de fármacos quimioterapêuticos, para demonstrar a sua elevada capacidade de promover a atividade de fármacos nas células cancerígenas do pulmão. Foi demonstrado que a região N-terminal do péptido pode ser associada à sua entrada preferencial, enquanto a sua região C-terminal estará mais associada à atividade citotóxica. O primeiro objetivo desta tese era a funcionalização de nanopartículas poliméricas com a região N-terminal do p28 contendo os primeiros 18 aminoácidos (péptido p18), para quantificar a interação de NPs funcionalizadas com o p18 com células A549 de cancro do pulmão. Para o segundo objetivo, foi feita uma nova experiência com PLGA-p28-NPs para estudar o seu efeito ao nível da organização da membrana plasmática das células cancerígenas, quando estas são tratadas com 4 condições diferentes: NPs funcionalizadas (250 µg/mL); NPs não funcionalizadas (250 µg/mL); p28 livre (2,5 µM); p28 livre (50 µM). A avaliação foi possível com a utilização da sonda fluorescente Laurdan e uma microscopia de excitação de dois fotões.

Para a experiência com p18, a interação das NPs funcionalizadas e não funcionalizadas com p18 foi realizada em células do cancro do pulmão A549 e células humanas não-cancerígenas dos brônquios 16HBE14o- através de citometria de fluxo. Estes resultados foram comparados com os obtidos em estudos anteriores do p28 para ver se este novo fragmento de 18 aa traz alguma vantagem em termos de interação celular, e concluiu-se que o p18 não promove uma interação mais forte com as células do que o p28. No segundo objetivo desta tese, em cada condição observa-se uma diminuição na ordem da membrana plasmática quando comparada com o controlo. O p28 livre (2.5 µM) foi o tratamento que causou uma maior perturbação da membrana, reforçando o seu papel na possível diminuição do conteúdo de jangadas lipídicas (*lipid rafts*).

## PALAVRAS-CHAVE

Nanopartículas | p18 | p28 | Cancro | Laurdan

# TABLE OF CONTENTS

# LIST OF FIGURES

# LIST OF TABLES

# LIST OF ABBREVIATIONS

**Aa –** amino acid

**AuNPs** – gold nanoparticles

**BBB** – blood-brain barrier

**bPrPp** – bovine prion protein

**CAV1** – caveolin-1

**CE%** - conjugation efficiency percentage

**CNS** - central nervous system

**CNTs** – carbon nanotubes

**COP-1** - constitutive photomorphogenic 1

**CPPs** - cell penetrating peptides

**CRC** - colorectal cancer

**DBD** - deoxyribonucleic acid -binding domain

**DLS** - dynamic light scattering

**DMEM** - Dulbecco's Modified Eagle Medium

**DMF** - N,N-dimethylformamide

**DMSO** – dimethyl sulfoxide

**DNA** – deoxyribonucleic acid

**Dox** – doxorubicin

**DTX** – docetaxel

**ECACC** - European Collection of Authenticated Cell Cultures

**EGFR** - epidermal growth factor receptor

**EMT** - epithelial-to-mesenchymal transition

**Entap** - Enterococcal anti-proliferative peptide

**EPR** - enhanced permeation and retention

**FBS** - Fetal Bovine Serum

**FDA** – Food and Drug Administration

**GEF** – gefitinib

**Geo MFI –** geometric mean fluorescence intensity

**GP** – generalized polarization

**HCC** - hepatocellular carcinoma

**HIV-1** - human immunodeficiency virus type 1

**HNC** - head and neck cancer

**HPLC** – high performance liquid chromatography

**HSV-1** - Herpes simplex virus type I

**HUVEC** - human umbilical vein endothelial cells

**Iri** – Irinotecan

**K-FGF** - kaposi fibroblast-growth factor

**LDV** – laser doppler velocimetry

**LMWP** - Low molecular weight protamine

**Mal** – maleimide

**MDR** - multidrug resistance

**MEM** - Minimum Essential Medium

**MPEG** - methoxy poly(ethylene glycol)

**mRNA** – messenger ribonucleic acid

**MWNTs** - multi-walled carbon nanotubes

**NC** – negative control

**NDDSs** - nanosized drug delivery systems

**NIR** - near-infrared region

**NLS** - nuclear localization signal

**NP** – Nanoparticle

**f-NP** – functionalized nanoparticles

**nf-NP** – non-functionalized nanoparticles

**OSCC** - oral squamous cell carcinoma

**PBS** – phosphate-buffer saline

**PC** – positive control

**PCL** - poly(Ɛ-caprolactone)

**PD** - plasmid display

**PDI** - polydispersity index

**PEG** - poly(ethylene glycol)

**PEI** - percutaneous ethanol injection

**PFA** – paraformaldehyde

**PG-1** - protregin-1

**PLGA** - poly (lactic-co-glycolic acid)

**PNPs** – polymeric nanoparticles

**PTDs** - protein transduction domains

**PVP** - poly(vinyl pyrrolidone)

**QDs** – Quantum dots

**RFA** - radiofrequency ablation

**RGD** - arginylglycylaspartic acid

**RNA** – ribonucleic acid

**ROI** – regions of interest

**SELEX** - systematic evolution of ligands by exponential enrichment

**SERS** - surface-enhanced Raman spectroscopy

**siRNA** - small-interfering ribonucleic acid

**SLNs** – solid lipid nanoparticles

**SWNTs** - single-walled carbon nanotubes

**TACE** – chemoembolization

**TAT** - trans-acting activator of transcription

**TCEP** - tris(2-carboxyethyl) phosphine hydrochloride

**TFA** - trifluoroacetic acid

**VEC** - vascular endothelial-cadherin

**Z-average** – average size

# 1. STATE OF ART

## 1.1 Nanotechnology in Cancer Treatment and Diagnosis

One of the main diseases that endangers human life is cancer, and at the moment the main therapies still mostly consist of surgery, radiotherapy, and chemotherapy. However, because of their non-specific distribution throughout the body, these treatments can damage surrounding tissues and have a number of toxic side effects that are harmful to the patient by harming healthy cells. Drug resistance in cancer cells is another issue with chemotherapy medications. New cancer therapy methods must therefore be developed in order to get beyond these constraints [1].

Nanotechnology has been researched and improved in recent years in order to be employed in the treatment of cancer. Designing, synthesizing, characterizing, and using materials and technologies whose smallest functional organization is on the nanoscale (nm) scale is known as nanotechnology [2]. Through its use in the detection or treatment of diseases at the cellular level, nanotechnology has the potential to revolutionize the development and delivery of medical solutions [3]. As a result, this new field encouraged the creation of a nanoscale material, with a diameter ranging from 1 to 100 nm, which could be promising for the development of a new application for the treatment of cancer, as well as for its diagnosis, because they are small enough to be able to penetrate eukaryotic cell membranes. These nanosized materials are called nanoparticles (NPs).

NPs are nanocarriers that have a higher surface-to-volume ratio than conventional materials and are composed of three layers: surface layer, shell layer, and core [4]. In nanomedicine, they became efficient for therapies due to their unique properties, such as drug delivery, because NPs can carry drugs inside and protect them from degradation, which promotes developments in the treatment of cancer [5]. The unique properties of NPs are the size because it facilitates penetration over biological membranes and it extends bioavailability in tumor tissue, and the possibility to overcome toxic effects caused in healthy human cells by chemotherapeutic drugs by producing NPs with non-toxic materials [6].

Therefore, since the first approval by the U.S. Food and Drug Administration (FDA) of a liposomal nanomedicine for Kaposi sarcoma and ovarian cancer in the 90s, improvements have been made in the synthesis and characterization of engineered NPs for diagnosis and treatment of cancers [7]. The majority of NP-based treatments that have been approved for clinical purposes, until recently, involved spherical liposomes, however, scientists have been working on a widespread range of NPs varying in size, shape, hardness, material, and surface properties (Figure 1), which modifies its cellular uptake and biodistribution [7,8].

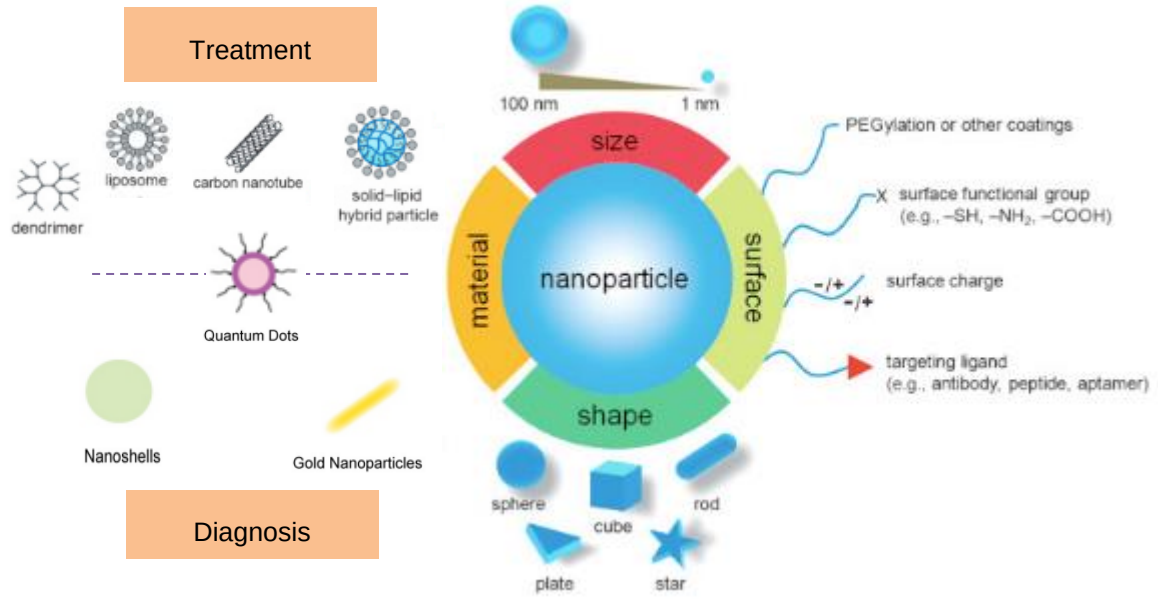


**Figure 1** - Nanoparticle categorized according to its size, shape, materials, and surface. Adapted from Heinz *et al.,* 2017 (doi: 10.1016/j.surfrep.2017.02.001).

### 1.1.1 Nanomaterials Utilized

In cancer treatment, these NPs are being used as a mode of transport for delivering drugs which can bring advantages such as a decrease in the side effects of the drug and an increase in the efficacy of the drug against the disease [9]. The NPs more commonly used are quantum dots (QDs), nanoshells, colloidal gold nanoparticles (AuNPs), liposomes, dendrimers, carbon nanotubes (CNTs), and polymeric nanoparticles (PNPs) (Figure 1) [9]. Nanoshells and colloidal AuNPs are usually used in cancer diagnosis while the rest is commonly used in cancer treatment, except for QDs which have been reported for both cases.

## Quantum Dots

QDs are small particles overcoated by a cap and a shell, which is the physical barrier in separating the core from the surrounding medium, allowing improved solubility, with a size between 2-10 nm [10]. During the QDs synthesis, the organic surfactants used are grown and form ligands on the surface of the core [11]. Over the years, several techniques based on QDs have been developed, one of them being the QD immunostaining, in addition to being more accurate than traditional immunochemical methods, it is a potential tool for the detection of tumor biomarkers [12]. QDs can also be used as a carrier to deliver drugs and can gather in specific parts of the body transferring the drug to those parts. An advantage they have is the ability to concentrate in a single internal organ, which makes them a possible solution against untargeted drug delivery, and can avoid the side effects of chemotherapy [9].

## Nanoshells

Nanoshells have a size between 10-300 nm, are composed of silica, coated with a metallic layer that is usually gold, and have a dielectric core. One of their properties is a strong optical absorption that is due to the electronic response of the metal to light, and this response depends on the size of the core and the thickness of the gold layer. Depending on the size of the particle, gold nanoshells can be produced to scatter or absorb light [13].

## Colloidal Gold Nanoparticles

AuNPs have a small size, good biocompatibility, and high atomic number which makes them a good contrast agent [9]. Studies demonstrate that AuNPs work in both active and passive ways to target cells. The passive targeting is regulated by a gathering of the gold NPs to enhance imaging because of the permeability tension effect in tumor tissues [9]. The active targeting is mediated by the coupling of AuNPs with tumor-specific targeting moieties, such as epidermal growth factor receptor (EGFR) monoclonal antibodies, to achieve AuNP active targeting of tumor cells [9]. Both passive and active targeting will be explained in detail in point 1.1.3. Main Drug Delivery Methods with Nanoparticles.

## Liposomes

Liposomes are closed vesicles composed of natural or synthesized phospholipid bilayer membrane and water phase nuclei, its size is usually bigger than 20 nm [14]. There are two kinds of liposomes, monolayer and multilayer liposomes. Hydrophilic drugs stay in the monolayer liposomes while hydrophobic drugs form before the multilayer liposome, which is due to the amphiphilicity of phospholipids that forms liposomes spontaneously [15,16]. Liposomes can be used as a drug delivery mechanism which consists of the combination of saturated drugs with organic solvents to form liposomes. These liposomes then can reach their site of action going from the bloodstream to the interstitial space and can target specific tissues through passive targeting strategy, and also active targeting upon the addition of targeting moieties to the outer surface of the lipid bilayer [15]. The liposomes that are smaller (20 nm) can penetrate the tumor cells more easily and have a bigger lifespan than larger liposomes because there are more changes for the latter to be recognized by the mononuclear phagocyte system [9].

## Dendrimers

Dendrimers have a spherical polymer core with branches composed of a central core, repetitive branching units, and terminal groups. These three main components can provide modifiable surface functionalities, which gives them an elevated level of control over their architecture and makes

them useful for drug delivery applications [17]. There are two routes to synthesize dendrimers: divergent [18] and convergent methods [19]. In the divergent method, the dendrimers grow from the nucleus towards the edges by adding monomers in layers. An advantage of this method is that at the end of the synthesis reaction the surface of the dendrimer can be modified with desired functional groups, and a disadvantage is that the purification requires a big period of time since the final product and the reagents used in the process have similar molecular weights, and other properties [20]. In the convergent method, the dendrimers grow from the edges towards the central nucleus, and, unlike the other method, this has an easier purification step because of the differences between the final product and the initial reagents. However, the yield is low and there are difficulties in obtaining higher generations of dendrimers due to steric interferences faced when the branches are connected to the central nucleus. Consequently, the divergent strategy is the most utilized for dendrimers synthesis [17,20].

## Carbon Nanotubes

CNTs consist of graphene that is rolled in sheets and can be categorized into two types based on their diameter and structure: single-walled CNTs (SWNTs) and multi-walled CNTs (MWNTs). As the name suggests, SWNTs only have one wall (tube), while MWNTs are composed of multi-walls that can slide against one another and concentric graphene [21]. CNTs in general have specific physical and chemical assets, such as surface area and mechanical strength, which makes them an excellent candidate for biomedical applications [9].

In order to target tumor cells, CNTs have the ability to absorb light from the near-infrared region (NIR), which causes the nanotubes to heat up due to the thermal effect [9]. There are multiple ways to make CNTs, and different producers employ different carbon sources, catalytic metals, and processing parameters including pressure and temperature [21]. Additionally, these nanocarriers can deliver different therapeutic compounds into living cells, particularly cancer cells [22].

## Polymeric Nanoparticles

PNPs have a particle size range of 10-100 nm [9], are known as polymer nanoparticles, nanospheres, nanocapsules, or polymer micelles, and they were the first polymers reported for drug delivery systems. PNPs are composed of two domains, a drug-loading core and a hydrophilic shell [23]. PNPs serve as drug carriers for hydrophobic drugs because of a covalent bond or the interaction via a hydrophobic core, and, to carry hydrophilic charged molecules, such as proteins, peptides, and nucleic acids, blocks are switched to allow interactions in the core and neutralize the charge [23]. The hydrophobic macromolecules and drugs can be transferred to the center of the PNPs, therefore, the injection of PNPs suspension could achieve a therapeutic effect [24]. Moreover, PNPs can be considered an ideal candidate for vaccine delivery, cancer therapy, and targeted antibiotics delivery in

accordance with the polymer choice and capacity to adjust drug release from PNPs [25].

PNPs can be used in nanomedicine to treat cancer, but there are difficulties in getting drugs to the target site with minimal side effects or drug resistance. However, recently, PNPs have been widely used in the design of nanotechnology-based cancer drugs because of their excellent potential benefits for patient care. Its usage is however constrained by adverse effects such as toxicity and cardiac issues [9]. Either by direct monomeric polymerization or from pre-existed polymers, PNPs can be effectively formulated using techniques like solvent evaporation, salting-out, supercritical fluid technology, and dialysis techniques. These techniques take advantage of a supercritical solution's quick expansibility into a solvent (liquid) or on its own, which can be used for PNP formulation from pre-existing polymers [25]. The most used techniques for PNPs preparations will be discussed briefly.

## Solvent Evaporation

In this procedure, polymeric emulsions are prepared from polymer dissolution in a volatile solvent, such as ethyl acetate which is preferred for safety and toxicological causes [26]. Then, the emulsion is transformed into NPs suspension by solvent self-evaporation, and the polymers used are allowed to disperse through the emulsion continuous phase [25,26]. Evaporation of the solvent was granted by pressure reduction or continuous stirring at room temperature [25]. Moreover, the designed NPs can be picked up and collected by ultracentrifugation and, subsequently, produced NPs can be lyophilized [27].

## Emulsion polymerization

Emulsion polymerization is the method that is most frequently used to manufacture PNPs from monomers because it offers the benefit of employing water as a dispersion medium, which is ideal for safety and an excellent heat removal control during the polymerization process [25]. This technique falls within the categories of conventional and surfactant-free emulsion polymerization [28,29]. The surfactant-free approach uses monomers, a water-soluble initiator, and deionized water to conduct the polymerization process without the usage of an emulsifier. A water-soluble initiator agent, surfactant, a monomer that isn't very water-soluble, and water are the ingredients used in the traditional approach [25]. Due to the surfactant's interaction with a free radical, both procedures begin when the monomer disperses in the continuous phase. A difference between the two methods is dependent on the monomer aqueous solubility [30].

## Nanoprecipitation

This low-energy method makes it possible to produce NPs with the desired features and functionalities. The emulsification can be done without the use of surfactants or high-shear force approaches. The spontaneous emulsification process is triggered by solvent shifting without precursor

emulsion. In a typical procedure, a hydrophobic solute is dissolved in a solvent wherein they have high solubility, and after mixing with water, the medium turns into a non-solvent for the solute. This causes the solute to become super-saturated, phase separate from the solution, and produce NPs in a predictable and controllable way. Without the addition of surfactants, the homogenous dispersions produced by nanoprecipitation typically display remarkable stability for days or even months. Since nanoprecipitation requires no external energy input and can produce controlled-property NPs in a single step, it has numerous advantages over other processes. As a result, it is frequently viewed as a cost-effective but efficient and adaptable approach for manufacturing NPs [31,32].

In table 1, we can observe a brief summary in relation to the previously mentioned nanomaterials.

**Table 1** - Types of nanomaterials utilized in the treatment and diagnosis of cancer, their advantages, limitation, and size in nm (nanometers).

| Class of Nanomaterial | Advantages | Limitations | Size (nm) |
|---|---|---|---|
| **Quantum Dots (QDs)** | High fluorescence intensity; long lifetime; good resistance to photobleaching [33] | Quantifying any QD signal in deep tissues based on fluorescence alone is challenging [33] | 2-10 [10] |
| **Nanoshells** | Non-toxicity; biocompatibility; bio sensing application [34] | Hardly travel the long distance from superficial blood vessels to deep tumor sites due to size limitations [35] | 10-300 [13] |
| **Colloidal Gold Nanoparticles** | Minimal invasiveness; no cumulative toxicity; reduced morbidity [36] | Toxicity; size and biodistribution; cost of synthesis [36] | 10-30 [36] |
| **Liposomes** | Amphiphilic; generally biocompatible; protect drugs from degradation [37] | Large size, limited stability [37] | >20 [14] |
| **Dendrimers** | High degree of loading of the active drug molecules, through | In drug delivery, the higher the generation of poly(propylene imine), | <10 [17] |

| | | | |
|---|---|---|---|
| | physical or chemical interactions [38] | the higher the hemolytic toxicity [17] | |
| **Carbon Nanotubes (CNTs)** | Improves mechanical strength; excellent reinforcing material which can control crack propagation [21] | If CNTs are not dispersed well in a matrix the benefits of using this material will be limited and defects could occur [21] | 10-100 [21] |
| **Polymeric nanoparticles (PNPs)** | Easily modified; generally small size; biocompatible [37] | Limited stability [37] | 10-100 [9] |

### 1.1.2 Surface Modifications of Nanoparticles

When NPs contact a biological fluid, their surface will be covered with biological macromolecules, as serum proteins absorb onto a NP surface (opsonization), therefore, the *in vivo* trafficking, uptake, and clearance of NPs are changed [39]. For instance, polymers attached to the particle surface, e.g., poly(ethylene glycol) (PEG), or poly(vinyl pyrrolidone) (PVP), are often used to increase NPs stability in suspensions. PEG, a polymer to coat a NP surface, reduces nonspecific adsorption of serum proteins and minimizes the formation of protein agglomeration, which increases the circulating time of the NP [39]. PEGylation is a process of the attachment of PEG polymer chains to molecules, and this process of various nanomaterials, such as NPs, results in a longer circulation time in the blood [40]. PEG enables not only the selective attachment onto NP surfaces, but also confers multiple possibilities for further biofunctionalizations, for instance, terminal functional moieties such as carboxylic (-COOH) and amine (-$NH_2$) groups that are widely used because they can be introduced into PEG molecules without deteriorating the colloidal stability of the pegylated NPs in blood and plasma [41].

Zwitterionic ligands are molecules with two or more functional groups that have a net charge of zero, mixed positive and negative charges, and are therefore less sensitive to strong ionic solvents. They have thus been investigated as excellent ligands for NP stability in biofluids. According to reports, these ligands produce NPs with substantially lower degrees of opsonization and hydrodynamic ranges than polymers like PEG [41]. However, zwitterionic NPs' surface charge distribution can affect their uptake and biodistribution. It has been reported that zwitterionic NPs with positive surface charges exhibit non-specific adsorption *in vitro* and *in vivo*, whereas those with negative surface charges are less likely to interact with proteins [42]. Another kind of ligand is the targeting ligand. A category that comprises substances including peptides, aptamers, and antibodies. Because they connect to receptors in the cell plasma membrane, these ligands are used in a variety of

functionalization strategies that can provide colloidal stability in biological media and help to a more specific interaction of the NPs with cells. Additionally, if these NPs are encapsulated with a drug, it can provide a more precise drug delivery system (Figure 1) [41].

### 1.1.3 Main Drug Delivery Methods with Nanoparticles

NPs are able to exploit the distinct cancer pathology and its molecular biology to result in higher uptake and preferential targeting of therapeutics to the tumor compared to traditional treatments, this is achieved by two methods, 'passive' or 'active' targeting [43] (Figure 2). Interactions between NPs and blood proteins, penetration into solid tumors, and optimized active (vs passive) targeting for diagnosis of cancer constitute the main clinical application barriers but, fortunately, many developments associated with these aspects have been achieved [39].

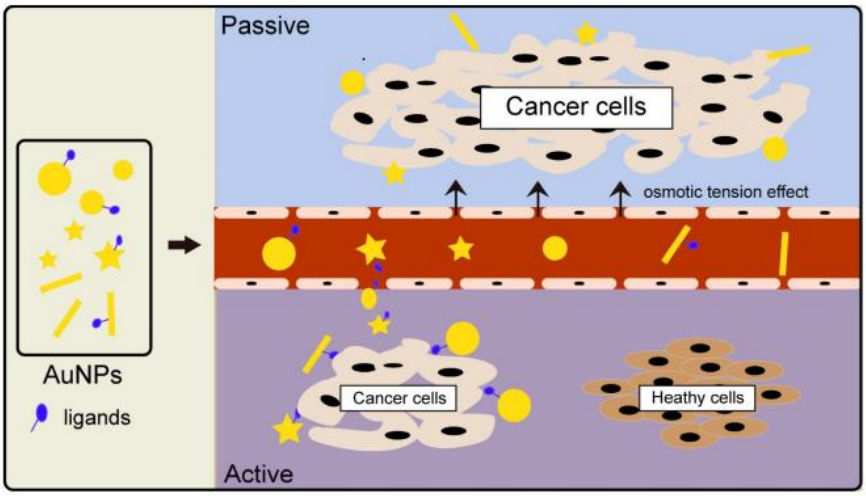


**Figure 2** - Types of gold nanoparticles (AuNPs) with different sizes and ligands accumulating in tumor tissues by the action of osmotic tension effect (passive targeting) or localized to specific cancer cells in a ligand-receptor binding way (active targeting). Source: Jin *et al*., 2020 (doi: 10.7150/ijms.49801).

## Passive Targeting/Enhanced Permeation and Retention Effect

Passive targeting refers to NPs' preferred extravasation ability from the bloodstream into tumor tissue, with a size range of 10-150 nm [39]. This occurs because the tight junctions between endothelial cells in new blood vessels in tumors might become loose and permeable because they do not develop properly. Because of this, NPs can cross these porous connections and gather in tumor tissue [44]. The osmotic tension effect, also known as the enhanced permeation and retention (EPR) effect, is a method of the NPs entering the tumor passively [45]. When creating NP probes for a larger accumulation in tumors, the parameters of the NPs, specifically their size and form, should be taken

into account [39]. However, these studies can have many limitations, including the lack of control in the uptake that can result in off-target drug delivery and drug resistance. As well as the fact that some tumors do not exhibit a strong EPR effect, and the permeability of the blood vessels can vary throughout the tumor tissue [43]. To address this, it is necessary to design nanosystems with active-targeting ligands or stimuli-responsive characteristics [46].

## Active Targeting

In addition to passive targeting based on the EPR effect and to overcome its limitations, there is a large number of studies on methods that help the identification of receptors on the cell surface for the active targeting of tumor tissues [39]. So, active targeting is where a targeting ligand is introduced onto the surface of the NP to target specific changes in cancer cells. Changes that healthy cells and tissues do not have. The process where we bind a ligand into the NP is called the functionalization of NPs. In this process, NPs will recognize and bind to target cancer cells through ligand-receptor interactions, and the NPs are internalized before the drug is released inside the cell, resulting in less off-target drug release compared to the passive targeting system [43].

By increasing the number of NPs given to tumor tissue per unit of time, this technique improves the sensitivity of *in vivo* tumor detection techniques [47]. Binding the NP to cell membrane receptors overexpressed in cancer cell lines, such as the EGFR, is one method of achieving this targeting. This receptor has been linked to the aggressiveness of numerous cancers, including non-small cell lung, renal, ovarian, and colon cancers [43]. Active targeting performs better than passive targeting for the early detection of cancers using high contrast imaging [39]. Preclinical research has focused on a variety of polymeric NP designs and targeting ligands, including small molecules, polypeptides, protein domains, antibodies, and nucleic acid aptamers that can be coupled with other substances like fluorescent dyes and carbohydrates (Figure 3) [48,49].

### Aptamers

Aptamers are created from chemically manufactured short-stranded DNA or RNA oligonucleotides, or peptide sequences chosen by a procedure known as SELEX (systematic evolution of ligands by exponential enrichment) [50]. They are nontoxic, low-molecular-weight targeting ligands without inherent immunogenicity. Because they may regain their active conformation even after thermal denaturation, they are more adaptable and stable than natural antibodies. The NP-aptamer conjugate approach has created aptamers that are efficiently transported to a particular target region in tumor cells, where they bind with high affinity and overexpress receptors on target cells by folding into complex three-dimensional structures [50].

### Peptides

The most famous and used targeting ligand for cancer therapies are small internalizing peptides because they have the advantage of being synthesized on a large scale with excellent quality

control and a low cost, and, usually, can be more stable than antibodies due to their small size and improbable to be immunogenic [51,52]. An example is a study that used a peptide for active targeting of tumor tissues *in vivo*, in which the arginylglycylaspartic acid (RGD) peptide is recognized by a receptor (integrin αvβ3) that is on the cell surface and involved in cancer angiogenesis and metastasis [53]. Most of these peptides not only can be used as targeting ligands, but they can also internalize cells, called cell penetrating peptides (CPPs), which allows an even more specific drug delivery in case we conjugate drug-encapsulated NPs with these CPPs to penetrate human cancer cells.

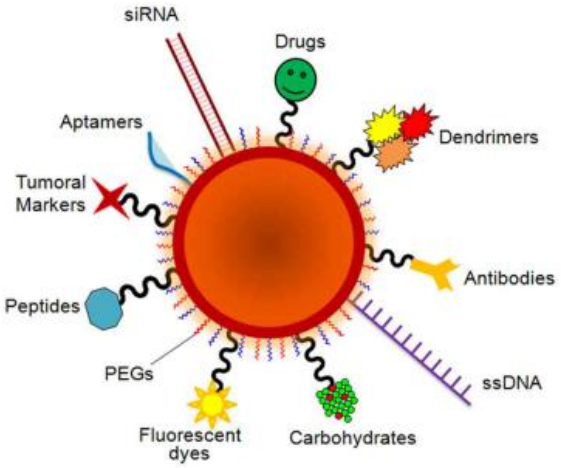


**Figure 3** - Representation of a multifunctional Nanoparticle. RNA and DNA bound by colorimetric assays can be used for gene silencing. Fluorescent dyes can be bound to the surface and used as reporter molecules or contrast agents. Carbohydrates may be useful as sensitive colorimetric probes. PEG is used to improve solubility and decrease immunogenicity. Tumor markers, peptides, carbohydrates, polymers, and antibodies can also be used to improve nanocarrier distribution, effectiveness, and selectivity. Aptamers and anticancer drug molecules are also used for delivery to the target tissue. Source: Conde *et al.* 2014. (Doi: 10.3389/fchem.2014.00048).

## 1.2 Cell-penetrating Peptides

The cell membrane is a semipermeable barrier that serves as a protective layer for the cells, and it only allows the transport of compounds with small molecular sizes, which can be transported using channels and specific carriers [54]. However, macromolecules are unable to use these modes of entry, especially macromolecules used for therapeutic purposes, such as proteins, peptides, and nucleic acids [55]. Therefore, some obstacles need to be overcome, such as the limited cellular uptake and low target specificity of these molecules, and, in order to do so, the need for new delivery and administration strategies has increased [56].

Positively charged small peptides with 5–30 amino acids (aa) in length, known as CPPs or protein transduction domains (PTDs), can pass through biological membranes and transfer a range of substances into cells [57]. CPPs are a viable candidate for intracellular delivery because they have a

peptide sequence that identifies a cell membrane receptor, have low cytotoxicity, do not trigger an immune response, and have a high transduction efficiency (internalization efficiency of CPPs into a cellular membrane) [57]. When cargo molecules are attached to the CPP, the intact cargos penetrate and are subsequently internalized by cells [58].

In the 80s, this group of peptides was first found with the discovery of the trans-acting activator of transcription (TAT) peptide, encoded by the human immunodeficiency virus type 1 (HIV-1), and it was shown that this peptide could enter cells and translocate into the nucleus [59]. In the 90s, it was discovered the neuronal cell internalization of the peptide penetratin, which is derived from the third helix of the Antennapedia homeodomain of *Drosophila melanogaster* [56]. Today, we have innumerable CPPs and databases to search existing CPPs based on chemical modifications, category, cargo, or peptide lengths [60]. CPPs can be divided into three categories: cationic, amphipathic, and hydrophobic (Figure 4) [54,61].

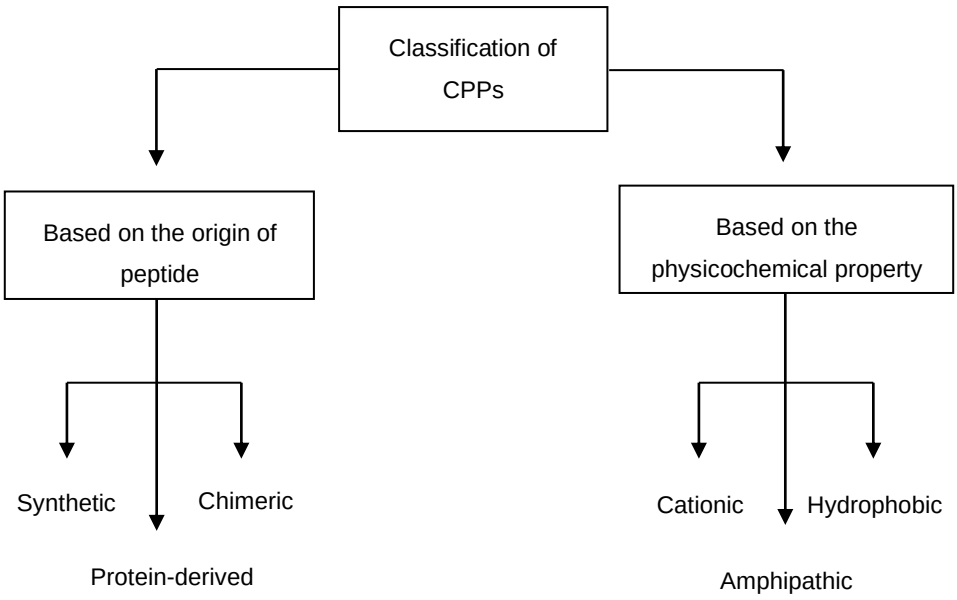


**Figure 4 -** Schematic diagram of various classifications of cell-penetrating peptides (CPPs). Source: Derakhshankhah *et al.,* 2018 (doi: 10.1016/j.biopha.2018.09.097).

## Cationic Peptides

Cationic peptides are a class of peptides derived from heparin-, DNA- and RNA-binding proteins that contains a high positive charge because of the high concentration of amino acids such as arginine, lysine, and histidine, which are positively charged [61 62]. The first-ever CPP derived from the HIV-1 protein Tat, mentioned before, is a cationic peptide, and the majority of these peptides are naturally occurring from peptide sequences, however, there exists artificial cationic peptides [54]. The designated amino acids give the cationic charge to the peptide and allow its interaction with anionic motifs on the plasma membrane by a receptor-independent mechanism [61]. Some of these cationic

peptides are being used for drug delivery in cancer treatments, mostly conjugated with a NP as a ligand, and this class of peptides need the presence of cell surface proteoglycans, due to their negative charge, to interact with the cell membrane through electrostatic interactions [63]. In Table 2, some of the cationic CPPs described in literature are represented.

**Table 2 -** Examples of cationic cell-penetrating peptides (CPPs).

| CPP | Sequence | Length (aa) | Origin | References |
|---|---|---|---|---|
| TAT | GRKKRRQRRRPPQ | 13 | HIV-1 Tat protein | [59,64] |
| Penetratin | RQIKIWFQNRRMKWKK | 16 | *Drosophila* Antennapedia homeodomain | [65] |
| LMWP | VSRRRRRRGGRRRR | 14 | Protamine Sulfate obtained from fish | [66] |
| Polyarginines | R(n); 6 < n < 12 | 6-12 | Synthetic | [67] |
| SynB1 | RGGRLSYSRRRFSTSTGR | 18 | Protegrin-1 isolated from porcine leukocyte cells | [68] |
| KT2 | NGVQPKYKWWKWWKKWW | 17 | Synthetic | [69] |

As it has been mentioned before, the first CPP discovered is the TAT peptide [59,64]. Covalently, the conjugation of TAT peptide (or a specific peptide sequence of it) to proteins or fluorescent markers allows these molecules to enter the cell and target the cell nucleus, which results in target gene expression [70].

Low molecular weight protamine (LMWP) peptide derives from protamine sulfate and it was discovered in 1999 [66]. Protamine sulfate is the clinical antagonist to heparin and is used after cardiovascular surgery to neutralize the anticoagulant function of heparin, however, its use is associated with adverse effects such as idiosyncratic fatal reactions [66]. To resolve this issue, studies found that heparin coagulation may only require a small arginine-rich fragment of protamine, which was proven by developing the LMWP peptide fragment by enzymatic digestion of protamine sulfate

using thermolysin [66]. *In vitro* studies reported a great success that LMWP could completely neutralize the anticoagulant functions of heparin. In terms of the toxicity evaluation of LMWP, it has less toxicity than TAT peptide [71].

Several articles proved that the internalization of cationic CPPs relies on the presence of arginine residues, which are thought to interact with anionic cell surface proteoglycans [72]. An example of this event is the internalization of polyarginines, which was proven that peptides containing a high percentage of arginine amino acids have the ability to cross the plasma membrane of cells [73]. The cell uptake increases with the increase of the peptide length, however, polyarginines longer than 16 aa are more cytotoxic [67].

In 1993, a family of small cysteine-rich peptides was discovered, designated as protregin-1 (PG-1) [74]. This peptide was able to cross the mammalian cell membrane, but it had the limitation of provoking cell lysis which led to necrosis or programmed cell death. Therefore, PG-1 was modified by replacing the cysteines with serines, which led to the formation of linear peptides (SynB vectors) that still maintain the advantage of crossing the cell membranes but it does not trigger cell lysis [75,76]. SynB vectors can be used to enhance brain uptake of doxorubicin, a chemotherapeutic drug, without compromising the integrity of the tight junctions, which is an effective delivery mechanism for carrying drugs across the blood-brain barrier (BBB) and can be used for the treatment of brain tumors. This reinforces the usefulness of peptide-mediated strategies for improving the availability and efficacy of central nervous system (CNS) drugs [76].

The synthetic KT2 peptide, derived from the peptide sequence of Luecronin I, has good antibacterial activity against three bacterial strains, such as *Staphylococcus epidermidis* ATCC 12228, *Salmonella typhi* DMST 22842, and *Escherichia coli* ATCC 25922 [69]. However, it was discovered that it promotes anticancer effects in cervical cancer and human colon cancer cells. A study showed that KT2 has a high uptake efficiency because it has the ability to enter the cell membrane and accumulate in the cytoplasm [77]. KT2 peptide exhibit both time and concentration-dependent manner inhibiting the growth of human colon cancer cells, as well as inhibiting colony formation. This peptide shows no toxicity in human red blood cells and kidney epithelial cells, but it is still not well known the cytotoxic effects caused by this peptide in other normal cells of the human body [77].

## Hydrophobic CPPs

Only non-polar residues or a small number of charged amino acids (less than 20% of the sequence) are present in hydrophobic CPPs, which are formed from signal peptide sequences. The potential use and mechanism of hydrophobic CPP translocation are less well understood than those of cationic and amphipathic peptides [54]. For example, SG3 [63], Pep-7 [78], kaposi fibroblast-growth factor (K-FGF) [79], and C105Y [80] are CPPs that have already been described (Table 3). The peptide sequence of hydrophobic CPPs, in contrast to the majority of amphipathic or cationic CPPs, has no impact on cell absorption [81].

**Table 3 -** Examples of hydrophobic cell-penetrating peptides (CPPs).

| Peptide | Sequence | Length (aa) | Origin | References |
|---|---|---|---|---|
| K-FGF | AAVALLPAVLLALLAP | 16 | Kaposi Fibroblast Growth Factor (FGF) signal peptide | [79] |
| C105Y | CSIPPEVKFNPFVYLI | 16 | Carboxyl-terminal tail of α1-antitrypsin (α1-AT) | [80] |
| SG3 | RLSGMNEVLSFRWL | 14 | Synthetic | [63] |

K-FGF belongs to a family of heparin-binding polypeptides that are mitogenic for a variety of mesoderm- and neuroectoderm-derived cell lineages, are angiogenic, and are also thought to play a role in development [82]. This CPP is derived from the hydrophobic region of the nuclear transcription factor NF-kB, and this hydrophobic region is responsible for the interaction with lipid bilayers [79].

The synthetic peptide C105Y is a part of the protein α1-antitrypsin, corresponding to the residues 359-374, and enhances gene expression from DNA NPs [80]. This peptide has the ability to enter the cytoplasm, nucleus, and nucleolus of live cells very quickly. This happens due to its hydrophobic C-terminal sequence because this sequence can enter cells and go to the nucleus in the same way as the full-length C105Y. Therefore, the peptide that does not have this C-terminal sequence cannot internalize cells [80]. This CPP enters cells through a pathway independent of clathrin and caveolae and enters the nucleus and nucleolus by nondegradative pathways. C105Y is a good candidate to deliver therapeutic cargoes, such as antivirals and tumor suppressors [80].

In 2011, it was identified a CPP by using a plasmid display from a randomized peptide library after four rounds of selection on PC12 cells, known as SG3 [63]. The mechanism of cell penetration of SG3 does not involve an electrostatic interaction with cell surface GAGs. This hydrophobic CPP is not toxic, the reason why it can be used for the delivery of anticancer agents [63].

## Amphipathic CPPs

Amphipathic CPPs are chimeric peptides and several are obtained by the covalent connection of a hydrophobic domain to a nuclear localization signal (NLS), such as MAP and MPG sequences [83]. For example, MPG is based on the SV40 NLS PKKRKV, and the hydrophobic domain is derived from the fusion sequence of the HIV glycoprotein 41 [84]. There are also amphipathic CPPs derived from

natural proteins, such as pVEC [85], ARF (1-22) [86], and BPrPp (1-30) [87]. Amphipathic α-helical CPPs have a hydrophobic patch on one side, whereas the other side can be cationic, anionic, or polar. An amphipathic β-sheet peptide is developed based on one hydrophobic and one hydrophilic stretch of amino acids exposed to the solvent [54]. Studies on VT5, an amphipathic peptide, have shown that the formation of β-sheets is essential for its cellular uptake [88]. Some amphipathic CPPs described in the literature can be observed in Table 4.

**Table 4** - Examples of amphipathic cell-penetrating peptides (CPPs).

| CPP | Sequence | Length (aa) | Origin | References |
|---|---|---|---|---|
| MPG | GALFLGFLGAAGSTMGAWSQPKK KRKV | 27 | Synthetic | [89] |
| pVEC | LLIILRRRIRKQAHAHSK | 18 | Murine sequence of the cell adhesion molecule VEC | [90] |
| p28 | STAADMQGVVTDGMASGLDKDY LKPDD | 28 | Azurin protein, *Pseudomonas aeruginosa* | [91] |
| BPrPp | MVKSKIGSWILVLFVAMWSDVGL CKKRPK | 30 | Bovine prion protein | [87] |
| RLW | RLWMRWYSPRTRAYG | 15 | Synthetic | [92] |

As it was mentioned before, MPG is a peptide created by using a flexible peptide linker to join the hydrophobic fusion sequence of HIV-1 glycoprotein 41 with the cationic NLS of SV40 large T antigen [89]. In the early years, it was used to deliver oligonucleotides and plasmid DNA into a cultured cell, but after a few years, a point mutation was introduced to the NLS to optimize the peptide for siRNA delivery. Consequently, it facilitates NP accumulation and siRNA release into the cytoplasm [93]. *In vitro*, the use of this peptide was successful for gene delivery for a variety of cell lines, but *in vivo* the endosomal entrapment was a limitation to transfection efficiency [72]. This issue was addressed by Crombez *et al*. that functionalized an MPG derivative with cholesterol and demonstrated that this

modification improved tissue distribution following systemic administration in mice [94].

An amphipathic CPP derived from murine vascular endothelial-cadherin (VEC) proteins was discovered in 2001, which is capable to cross cell membranes, pVEC [90]. The peptide sequence contains the 13 cytosolic amino acid residues closest to the membrane and five amino acids from the C-terminal of the transmembrane region [90]. The VE-cadherin protein-peptide VEC is translocated into living cells, and the sequence of pVEC contains a hydrophobic part (N- terminal) of five amino acids and a hydrophilic (C-terminal), positively charged part, from the cytosolic tail of the VE-cadherin. The basic residues of cell translocating peptides have been suggested to be important for electrostatic interactions with the negatively charged head groups of lipids in the plasma membrane, moreover, the sequence of pVEC has an amphipathic character, which also has been suggested as an important factor for cellular internalization [90]. This CPP is capable of delivering some proteins and oligomers to mammalian cells, which are through the hydrophobic domain and the cationic middle part of pVEC that are responsible for the cell uptake [95].

A peptide derived from the N-terminal of the unprocessed bovine prion protein (bPrPp), incorporating the hydrophobic signal sequence and a basic domain (N-terminal), internalizes into mammalian cells, even when coupled to a sizeable cargo [87]. Studies indicate that the internalization of this peptide is mainly through macropinocytosis, a non-selective form of fluid-phase endocytosis process, initiated by binding to cell-surface proteoglycans, and can transport large anionic cargo, such as DNA plasmid. bPrPP induces expression of a complexed luciferase-encoding DNA plasmid, demonstrating the peptide's ability to transport the cargo across the endosomal membrane and into the cytosol and nucleus [87].

In 2012, a CPP that possesses both cell-penetrating property and specific cell selectivity using mRNA display technology was synthesized, and designed as RLW peptide or CPP3 [92]. RLW peptide showed preferential penetration towards A549 lung human cancer cells and poor penetration towards normal human fibroblasts [92]. However, the application of this kind of peptide has not been evaluated yet, and the potential superiority over traditional CPPs needed to be further explored [96]. A study demonstrated that RLW could specifically improve the penetration ability of NPs on A549 cells rather than human umbilical vein endothelial cells (HUVEC), showing cell selectivity [96]. However, the application of this kind of peptides has not been evaluated, and the potential superiority over traditional CPPs needed to be further explored [96].

### 1.2.1 p28, Peptide Derived from the Azurin Protein

In 2002, it was discovered the protein azurin by Yamada *et al.* which is a bacterial redox protein with the capability to enter human cancer cells and induce apoptosis. It was reported that this protein promoted more cytotoxic effects in tumor tissues than in healthy ones [97]. Azurin is a 128-amino acid (14-kDa) copper-containing member of the cupredoxin family secreted from *Pseudomonas aeruginosa*, and it has been reported that it preferentially enters cancer cells more than similar normal human cells through endocytotic, caveosome-directed, and caveosome-independent pathways. After

entering cancer cells, azurin inhibits the growth of tumor cells which leads to cell shrinkage and death via binding to the DNA-binding domain (DBD) of the tumor-suppressor protein p53 and anti-proliferative and pro-apoptotic activity [98].

Due to its PTD, azurin has the ability to penetrate cells, and its peptide p28 (amino acids $Leu^{50}$-$Asp^{77}$) appears to function as both the PTD and an efficient inhibitor of cancer cell proliferation. The N-terminal (hydrophobic domain) of p28 is responsible for entry into human cells, whereas the C-terminal (hydrophilic domain) is in charge of p28's antiproliferative activity [91]. According to available data, p28 enters cells via an endocytic process driven by receptors that involves caveolin-1 (Cav1), the Golgi complex, and ganglioside GM-1. It is believed that the primary reason p28 preferentially accesses tumor cells over normal ones is because cancer cells have more caveolin receptors than normal cells and express these receptors at higher levels on the membrane of cancer cells. Evidence also suggests that p28 and azurin are energy-dependent, independent of membrane-bound glycosaminoglycans, depending on plasma membrane cholesterol levels, and do not require the integrity of the membrane to be disrupted. As a result, increasing the amount of cholesterol in the cell membrane causes p28 to enter the cells more efficiently [98].

Following cellular entry, p28 mostly inhibits cell proliferation to suppress tumor growth by interfering with biological pathways, particularly the p53 signaling pathway. Being a transcription factor and tumor suppressor, the p53 protein is crucial for the advancement of the cell cycle, DNA damage repair, and apoptosis. Constitutive photomorphogenic 1 (COP-1), an E3 ubiquitin ligase, attaches to the DBD of p53 in cancer cells and inhibits p53's function. If p28 is present, however, this peptide binds to the DBD and prevents COP-1 from interacting with p53. This increases p53 levels and causes the formation of p28-p53 complexes, which then triggers the transcription of proapoptotic genes like *BAX* and *Noxa*, which can activate a caspase cascade and begin an apoptotic process. Alternatively, the complex can cause a cell cycle arrest at the G2 to M phase by inducing the expression of cell-cycle inhibitors like the genes *P21*, *P27*, and *FOXM1* (Figure 5) [98–100].

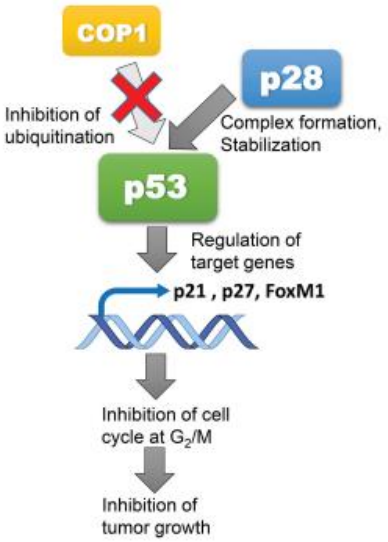


**Figure 5 -** Mechanism of the antitumor action of p28. p28 binds to the DNA binding domain of the p53 protein blocking COP-1-mediated proteasomal degradation of p53. The increase in the level and activity of p53 regulates the activity of the downstream genes, *P21, P27,* and *FOXM1*, leading to the inhibition of cancer cell cycle at G2/M and subsequent apoptosis. Source: Lulla *et al.,* 2016 (doi: 10.1093/neuonc/now047).

### 1.2.2 CPPs in Cancer Therapy

Consequently, CPPs could overcome the disadvantage present in cancer treatments used nowadays, which is why they are being tested and used for several applications such as drug delivery and imaging [101]. CPPs can be conjugated with various drugs via covalent and non-covalent attachments to serve as assistance in crossing otherwise impermeable biological barriers, especially the BBB [102]. The most common way for peptide-drug complexes to enter the cells is through endocytosis and the factors responsible for this uptake are drug and peptide concentrations, in combination with the structural properties of the plasma membrane [103]. However, in the peptide-drug complexes the drug is unprotected, and they can leak out before reaching the targeted site, which is inside cancer cells, and that is why encapsulation is commonly adopted in drug delivery systems, and one way to encapsulate these drugs is by using NPs.

NPs are increasingly being studied as multimodal platforms for the grafting of bioactive molecules useful for treatment. However, the inability to pass through the lipid membranes of cells limits their *in vitro* and *in vivo* use, so, to bypass this, CPPs can be conjugated in these bioactive molecules to facilitate cellular uptake, and to reduce side effects, such as cytotoxic effects. Moreover, due to the size of NPs, chemotherapeutic drugs can be encapsulated within these NPs. Polymeric NPs or even liposomes are typically used to develop a controlled release system, and this approach can be used to improve the distribution, absorption, and targeting of molecules, which otherwise would be eliminated or would not be able to reach the target tissue [104]. Several studies have been made for cancer therapy with NPs conjugated with CPPs and some of these studies are described in point 1.3. Nanoparticles Conjugated with CPPs for Cancer Therapy.

### 1.2.3 CPPs Derived from Microorganisms

From the CPPs mentioned before, only two are derived from microorganisms, those being the TAT peptide and p28 peptide, encoded by the human HIV-1 and *P. aeruginosa*, respectively. We can find a few microorganisms' CPPs in the literature, those being the α1H and α2H peptides, derived from *Yersinia enterocolitica* YopM effector protein, gH625 peptide, derived from glycoprotein H of Herpes simplex virus type I (HSV-1), Pep27anal2 peptide, derived from *Streptococcus pneumoniae*, and finally, Entap peptide, derived from *Enterococcus* spp.

The CPPs α1H and α2H, as well as TAT, are used to deliver the antibiotic gentamicin to target intracellular bacteria. The antibiotic gentamicin used to treat infections has a poor capability to cross eukaryotic cell membranes, thus, failing to reach therapeutic levels in intracellular bacterial infections. It is known that cell-penetrating recombinant YopM is functional and down-regulates the expression of pro-inflammatory cytokines, suggesting a dual of YopM as a delivery vehicle for cargo molecules and as a biological therapeutic for immunomodulation. The translocation ability is conferred by the two α-helices at the N-terminal, which acts as PTD, denoted α2H. It was shown that these CPPs can increase the intracellular delivery and the efficacy of gentamicin in killing intracellular pathogenic bacteria, therefore these CPPs can be applied to engineer very promising antimicrobial tools to treat infectious diseases. The α2H domain can deliver heterologous cargo into eukaryotic cells, therefore they could also be susceptible to use against these cells and in cancer therapy [105].

The peptide gH625 was characterized in 2005 and it is the HSV-1 peptide with the highest fusion capability and the most widely studied. gH625 is a membrane-perturbing domain, which interacts with biological membranes and is implicated in the merging of the viral envelope and the cellular membrane. The peptide has the capability to interact and destabilize target lipid membranes. gH625 cellular uptake is associated with its hydrophobic and amphipathic characters which provide the ability to interact with membrane lipids and to form a temporary helical structure that affects the organization of the membrane, therefore facilitating insertion into the membrane and translocation. It has been demonstrated that this CPP is able to cross the membrane bilayer and transport into the cytosol several compounds, such as liposomes, NPs, QDs, and proteins. Thereby, this peptide can be used against eukaryotic cells and also be applied in cancer therapy with drug delivery [106].

Pep27anal2 peptide constitutes an analog of the signal peptide of *S. pneumoniae* (Pep27). This substance activates this bacteria death program and exhibits antimicrobial properties. Pep27anal2 proved to be a more hydrophobic molecule than Pep27 and gets through the cell membrane inducing caspase- and cytochrome c-independent apoptosis. It has also been proved that it inhibits the proliferation of cell lines of leukemia, gastric cancer, and breast cancer. Enterococcal anti-proliferative peptide (Entap) is produced by clinical strains of *Enterococcus* sp. and has demonstrated antiproliferative activity against several cell lines of human gastric adenocarcinoma, colorectal adenocarcinoma, mammary gland adenocarcinoma, uterine cervix adenocarcinoma, and prostatic carcinoma. The antiproliferative activity of Entap in cancer cells is manifested by inhibition of their cell cycle at the phase of G1 and by induction of autophagous apoptosis [106].

## 1.3 Nanoparticles Conjugated with CPP for Cancer Therapy

As it was mentioned before, CPPs have emerged as flexible tools to enable drug delivery, and normally these peptide sequences are coupled to a biologically active cargo and can transport it across the plasma membrane [107]. On the other side, NPs provide an excellent opportunity in biomedical sciences and have been widely used to increase the pharmacokinetic properties of bioactive drugs, therefore, it is of extreme importance to increase cell penetration and delivery to intracellular target destinations of NPs by decorating them with CPPs [107]. Understanding the chemical interaction, the stability of formed bonds, and their influence on potential changes in physicochemical properties of CPPs and NPs are essential to developing conjugates that possess high cell internalization efficiencies and biocompatibilities [107]. Notably, due to their small size, some NPs are also able to cross the BBB and, thus, offer opportunities for the diagnosis and treatment of difficult-to-reach targets, such as brain tumors [108].

As it has been mentioned several times before, the standard chemotherapy regimen for treating cancer lacks specificity and frequently causes several negative side effects for patients. Studies with nanosystems of functionalized NPs with CPP encapsulated with cargo were conducted, and are currently being conducted, in an effort to get around these restrictions and produce a more effective treatment [60]. These constructions aim for the targeted treatment and elimination of tumors without harming healthy tissues. This has led to the study and development of several NPs conjugated with CPPs (Table 5) [60,109].

**Table 5 -** Conjugation strategies and different applications for cancer therapy.

| Construct | CPP | NP | Delivery Cargo | Application | Reference |
|---|---|---|---|---|---|
| AsTNP | TGN | PEG-PCL | DTX | Glioblastoma | [110] |
| MPEG-PCL-TAT + siRNA micelles | TAT | Methoxypoly (ethylene glycol) and poly (Ɛ-caprolactone) | siRNA | Brain cancer | [111] |
| CPP-LNP-siRNA | Arginine rich and siRNA carrier | Protamine-decorated lipid NP | siRNA GFP/luciferase | Melanoma cancer | [112] |
| AuNP/DOX/TAT/PEG/antibody | TAT-C | Au NP | DOX | Breast cancer | [113] |
| H+C-NPs | R9 | PLGA-PEG | PTX | Hepatic cancer | [114] |
| PLGA-LNP + miR139/afatinib | pH-sensitive CPP H and ligand R | Polymeric core to carry afatinib or miR-139 | Afatinib | Colorectal cancer | [115] |
| SLN-CMN and Lip-CMN | CMN | Liposomes and SLN | miR-200 or Iri | Head and neck cancer | [116] |
| p28-NPs-GEF | p28 | PLGA-PEG-Mal | GEF | Lung cancer | [117] |

In 2012, Gao *et al*. investigated the ability of the TGN peptide and the AS411 aptamer coupled with PEG-poly(-caprolactone) (PEG-PCL) NP to deliver the drug docetaxel (DTX) to mice with brain glioma. The TGN peptide was obtained through rounds of *in vivo* phage display screening from a 12-mer peptide library. Radiotherapy or chemotherapy, followed by surgical excision, is the typical course of treatment for brain gliomas, albeit it can be challenging to entirely remove the tumor. There is a need for targeting methods that are efficient for this type of cancer with a high BBB penetration because most chemotherapy has failed due to the rare BBB penetration and poor glioma targeting of the chemotherapeutics, and this study is an example of that [110]. The nucleolin protein, which is abundantly expressed in the plasma membrane of cancer cells, was able to attach to the DNA aptamers AS411, which are G-rich DNA aptamers, in this study, encouraging dual selectivity with TGN peptide. In this work, DTX was employed as a model drug to assess the anti-cancer effect. DTX is a highly potent inhibitor of microtubule depolymerization and has been used in the treatment of numerous malignancies, including brain tumors. Both TGN and AS1411 modified PEG-PCL NPs were used to create a cascade targeted delivery system (AsTNP). Increased survival rates in treated mice and improvements in anti-tumor activity when compared to saline and drug-free treated mice were used by the authors to demonstrate the efficacy of the treatment [110].

In 2013, a study made by Kanazawa *et al.* developed an efficient brain delivery system composed of nucleic acids, such as small-interfering RNA (siRNA). They evaluated the delivery of siRNA to the brain following intranasal administration with a methoxy poly(ethylene glycol) (MPEG)/polycaprolactone (PCL) copolymers conjugated with a CPP, TAT, carrier for the treatment of glioblastomas (MPEG-PCL-TAT) [111]. Glioblastomas are the most common types of intracranial tumors, and the standard therapy consists of cytoreductive surgery followed by radiotherapy, with a limited role for adjuvant chemotherapy, but, just like the study of Gao *et al.* mentioned above, the chemotherapeutic agents have a low efficacy due to the BBB, therefore, new therapeutic strategies are required to develop new candidate drugs and ensure delivery of these to the brain and CNS [111]. siRNAs are capable of silencing the expression of a defined gene and in cancer, this could be critical to cellular growth. Therefore, it is of interest to develop strategies that improve the delivery of these siRNAs to the brain, consequently, what Kanazawa *et al.* prepared was MPEG/PCL copolymers conjugated with TAT and evaluated the cellular uptake in rat neuron cells, RN33B cells, and the brain distribution of fluorescein-labeled dextran or siRNA by intranasal administration with MPEG-PCL-TAT in rats. The results showed that the MPEG-PCL-TAT, which was administered intranasally in rats, showed a higher brain transferability than that following intravenous administration of MPEG-PCL-TAT, suggesting that superior delivery of siRNA to the brain is possible. They also showed that the use of polymer micelles with surface-loaded TAT peptide for intranasal administration of nucleic acid enables the non-invasive supply of a therapeutic drug to the brain, due to the high rate of transfer of nucleic acid from the nasal cavity [111].

An arginine-rich protamine peptide was employed as a CPP and siRNA carrier in a study conducted by Asai *et al.* in 2014. The lipid derivatives of the peptide were created and used to create CPP-decorated lipid nanoparticles (CPP-LNP) that contain siRNA (CPP-LNP-siRNA) for potential melanoma cancer treatment. CPP-LNP-siRNA was internalized into B16F10 murine melanoma cells,

however because it was not associated with lysosomes, siRNA was transported from endosomes into the cytoplasm after internalization. This endosomal escape mechanism may be caused by the CPP's interaction with the endosomal membrane, which makes it easier to transport siRNA into the cytoplasm, or it may be caused by the CPP's role in the proton sponge effect. This could be the reason why the delivery of the siRNA to the cytoplasm happens very efficiently, resulting in the silencing of reporter genes [112].

Hossain *et al.* developed a study for breast cancer, in 2015, in which an *in situ* label-free intracellular drug release monitoring system based on biohybrid NPs was proposed. The biohybrid NP, consisting of a gold NP, a CPP, and a breast cancer-targeting antibody, was conjugated for facilitated specific cell targeting, increased uptake, and time-dependent intracellular anti-cancer drug release using surface-enhanced Raman spectroscopy (SERS). The cysteine-modified TAT peptide (TAT-C) was used as a CPP in the biohybrid NPs for increased uptake by the cancer cells and the anti-HER2 antibody was used to target the breast cancer cells (SK-BR-3) [113]. The biohybrid NPs were successfully conjugated with AuNP, TAT-C, PEG, and anti-HER2 antibody, and enhanced Raman signal of doxorubicin (Dox), the anti-cancer drug used, was loaded. The HER2-positive cancer cell (SK-BR-3) was specifically targeted with biohybrid NPs and showed the SERS signal of Dox from the entire cell and cell mortality increased to nearly 61% at 24 h with Dox-loaded biohybrid NP-treated cells, and there was no anti-cancer effect in unloaded biohybrid NP-treated cells, as it was expected [113].

Another type of cancer is hepatocellular carcinoma (HCC), which already has several therapeutic approaches such as surgery, radiofrequency ablation (RFA), percutaneous ethanol injection (PEI), and chemoembolization (TACE). However, these existing therapies are limited in terms of the cure and preventing metastases and relapses, therefore, chemotherapy remains to be the alternative treatment although it is not very effective [118,119]. Consequently, in 2018, Jin *et al.* developed and evaluated a work to improve HCC chemotherapy that uses paclitaxel-loaded NPs decorated with bivalent fragment HAb18 $F(ab')_2$ and polyarginine peptide [114]. Paclitaxel is a potent anti-cancer drug, especially cervical, breast, lung, and ovarian cancers, and there are many articles in the literature regarding the activity of paclitaxel against HCC *in vitro* and *in vivo.* Paclitaxel is traditionally intravenously administrated with cremophor EL as a solvent, however, this solvent may cause serious side-effects and lead to hypersensitivity reactions in many patients. Therefore, an albumin-bound paclitaxel NP is the first cremophor El-free paclitaxel agent which was approved for clinical application by the FDA [120]. Bivalent fragment HAb18 $F(ab')_2$ is a specific cancer-targeting antibody that recognizes and interacts with HAb18G overexpressed in HCC. Polyarginine is one of the most commonly used CPP and the combination of antibodies and CPPs in NPs can provide chemotherapy with cell specificity and enhanced uptake [114]. So, in this work, the construct H + C-NPs was developed by EDC/NHS chemistry for targeted delivery and effective endocytosis, and it was shown that drug-loaded NPs indicated cytotoxicity on HCC cells *in vitro* and *in vivo*. Specificity and higher uptake of H + C-NPs improved significantly and, overall, these results suggest that the multifunctional nanosystems with targeting and cell-penetrating abilities could become a potential gain for HCC chemotherapy [114].

Afatinib, a medication that inhibits tyrosine kinases, was utilized in the Hong *et al.* study from 2019 to prevent the phosphorylation of HER2 and HER3, which is linked to tumor resistance, metastasis, and invasion [115]. Clinical investigations have shown that increased EGFR expression is associated with tumor invasion and metastasis in 80% of patients with colorectal cancer (CRC), which leads to a poor response to conventional chemotherapeutics. In addition to EGFR, three additional HER2/neu (ErbB-2), HER3 (ErbB-3), and HER4 (ErbB-4) related ErbB/HER family receptor tyrosine kinases have been identified. It is known that pan-HER inhibitors like afatinib are effective against parental and resistant CRC cells, HER2-overexpressed CRC, and metastatic CRC [115]. Patients with non-small cell lung cancer who have the EGFR mutation can take the pan-ErbB inhibitor afatinib, which is orally active and irreversible. In human metastatic gastric cancer, mature miRNA-139 is downregulated in CRC, and overexpression of HER2 reduces miR-139 production and causes lymph node metastasis. In this study, a lipid-polymeric hybrid NP formulation for drug delivery was created. Lipids that had been modified with a targeting ligand and a pH-sensitive CPP H were used to decorate the NPs. The biological effects of these constructs on colorectal adenocarcinoma Caco-2 cells were assessed, and the results demonstrated an induction of apoptosis and an inhibition of Caco-2 cell resistance, suggesting that those multifunctional NPs may open the door to increasing colon cancer cells' sensitivity to afatinib [115].

Another cancer therapy that has been studied using NP decorated with CPPs is for the head and neck cancer (HNC), particularly oral squamous cell carcinoma (OSCC) developed by Lo *et al.* in 2020. A lot of the time OSCC is unresponsive to common chemotherapy and is usually accompanied by distant metastasis and poor prognosis, furthermore, therapy resistance has been observed in currently chemotherapeutics, and one of the reasons why is the epithelial-to-mesenchymal transition (EMT) and systemic toxicity caused by available antineoplastic agents. Irinotecan (Iri), a topoisomerase (Topo)-I inhibitor, induces cell death by inhibiting the relegation of double-strand DNA and it is normally pumped outside cancer cells by multidrug resistance (MDR)-associated proteins (MRPs). EMT contributes to the development of acquired Iri resistance and elevated migration and invasion in different cancer types, therefore, the capacity of current HNC therapies to suppress MDR and EMT is limited, thus, finding suitable therapeutics for co-treatment with Iri is needed to inhibit Iri resistance and increase the chemosensitivity of HNC to this drug [116].

One way to do it is by repressing EMT activation and this can happen with the help of a microRNA (miR) family called miR-200. The downregulation of miR-200 family members plays a key role in the anti-apoptosis, progression, invasion, and drug resistance of OSCC, thus, the authors decided to administrate miR-200 in solid lipid NPs (SLNs) and Iri in liposomes which can improve problems such as rapid degradation, limited tumor penetration, and low uptake into cancer cells. Both SLN and liposomes are decorated with three different CPPs, N peptide for tumor targeting, M peptide for mitochondrion directing, and C peptide for enhanced cancer penetration, making two constructs, SLN-CMN and Lip-CMN. Moreover, a PEG derivative was conjugated into lipid to form a pH-sensitive imine bond [116]. The results showed that the CPP and targeting peptides were exposed to improve the uptake and release of miR-200 and Iri into HNC human tongue squamous carcinoma and the functions of these NPs were: decreasing noncancerous cellular uptake through the protection provided

by the outer cleavable PEG-lipid shell; enhancing passive tumor targeting via the EPR effect; improving active tumor targeting via specific ligand-receptor binding. The apoptosis of the cancer cells treated was induced by regulating several pathways, such as the MDR, Wnt/β-catenin, and EMT pathways. In conclusion, this study suggested that chemo- and gene therapy co-treatment with pH-sensitive and targeting peptide-modified NP may be an advanced approach for HNC treatment [116].

Lastly, in our group, Garizo *et al.* developed a study in 2021 in which they used poly (lactic-co-glycolic acid) (PLGA) NPs functionalized with an azurin-derived peptide termed p28 and used as a drug the gefitinib (GEF), which is a tyrosine kinase inhibitor commonly used to treat various solid tumors expressing the EGFR, such as lung cancer. For this type of cancer, the common chemotherapeutic efficacy is also low due to the limited ability to reach the target cells, and this matter urged the development of new delivery strategies for the target release of drugs in an attempt to enhance their benefits, hence the development of this study [117]. The peptide p28 (28 amino acids) has preferential tumor cell internalization and anticancer activities making it an excellent molecule for nanosized drug delivery systems (NDDSs). Therefore, in gefitinib-loaded p28 functionalized PGLA NPs and, p28 improves the specific interaction of these NPs with A549 lung human cancer cells. Furthermore, p28-NPs containing GEF (p28-NPs-GEF) were able to specifically lower the metabolic activity of A549 cells while not affecting on non-tumor cells. *In vivo* the formulation p28-NPs-GEF decreased A549 primary tumor burden and the development of lung metastases. In conclusion, the progression of p28-functionalized NPs capable of penetrating cancer cell membranes while delivering GEF may provide a new strategy to improve lung cancer therapy [117].

## 1.4 Bacterial Vectors Associated with Cancer Treatment (Bacterio-robots)

Chemotherapy is the main therapeutic technique, as was previously said, however it is often deleterious owing to its potential side effects because it might occasionally fail to penetrate the tumor environment, lack selectivity, and kill normal cells. Using NPs conjugated with CPPs, as seen in previous sections, is one approach to get around this problem. However, bacteria also provide a number of advantages over currently used medications, and specific bacterial strains, such as *Clostridium*, in particular, proliferate well in tumor cells because they are highly active and motile in the anaerobic environments present in tumor cells [121].

The toxicity of bacteria at the required dosage level is the major barrier to their use as anticancer agents, but there have been studies on the genetic modification of bacteria to express genes of therapeutic interest, therefore these can serve as vehicles to carry anticancer agents like proteins, peptides, and enzymes. Similarly, bacterial ghosts can be utilized to deliver the requisite drugs to a specific site. Bacterial ghosts are non-denatured envelope-derived from gram-negative bacteria, which retain the original morphological and structural features of a normal bacterium [121]. One example is the site-specific delivery of Dox to human colorectal adenocarcinoma cells (Caco-2) using bacterial ghosts derived from *Mannheimia hemolytica*, and these exhibited strong anti-proliferative

activity against Caco-2 cells [122].

The combination of diagnostic and therapy for tumor evasion has come up with a technology for developing Bacteriorobots (bacteria-based microrobots), which can be loaded with peptides, antibodies, and nucleic acids having anti-tumor effects. The prototype of a bacteriorobot involves a combination of polystyrene bead and flagellated bacteria, and a bacteriorobot composed of *Salmonella typhimurium* attached to a microstructure containing drugs has been synthesized and enables the microstructure to move towards the tumor. This combination of robotics and biotechnology presents an interesting phase of anticancer therapy [121].

## 2. Thesis Outline

This thesis builds on previous work from our group exploring the biological role of the CPP p28 (28 aa) (LSTAADMQGVVTDGMASGLDKDYLKPDD-NH2) derived from the protein azurin (UniProt ID P00282). This peptide is localized in the alpha-helix region, within 50-77 aa, the domain responsible for azurin's antiproliferative activity, and it is also characterized as being amphipathic, which means it has a hydrophilic domain (50-66 aa) localized in the C-terminal, and a hydrophobic domain (67-77 aa), localized in the N-terminal (Figure 6) [98,123,124].

We recently developed a new nanosystem (p28-NPs-GEF) in which the p28 favored the internalization of the nanosystem in lung cancer cells, where GEF was released to exert its anticancer therapeutic activity. Thus. p28-functionalized NPs were capable of penetrating cancer cell membranes, while delivering GEF, providing a new strategy to improve lung cancer therapy [99].

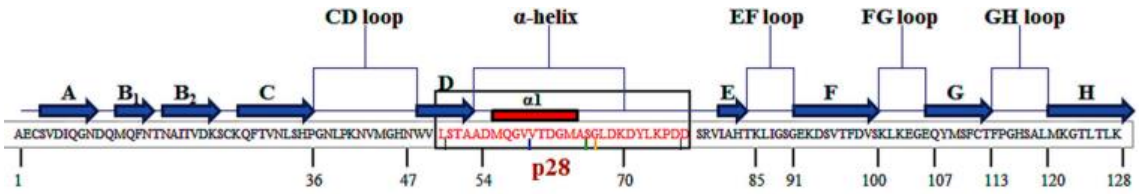


**Figure 6 -** Azurin's sequence (128 amino acids) and in the black box it is located the peptide p28 (28 amino acids) from amino acids 50-77. Source: Yaghoubi *et al.,* 2020 (doi: 10.3389/fonc.2020.01303).

Therefore, for the first objective of this work, we tested the interaction of similar nanosystem, but with a change on the CPP that instead of being the p28 peptide we utilized a smaller version of that same peptide called p18 peptide (60-77 aa of azurin), which has the same origin as p28. The difference between these two peptides, despite being the size, is that p18 does not have the cytotoxicity domain present in the C-terminal region like p28 has, therefore it only has the domain responsible for the preferential entry into cancer cells present in the N-terminal region (Figure 7). The advantages would be working with a much smaller peptide which is cheaper, it has a lower risk of degradation, and, hypothetically, smaller molecules have a higher affinity/specificity to target, lower toxicity profiles, and also a better tissue penetration [125]. Therefore, one of the objectives of this thesis was to see if there were advantages in using a much smaller peptide in terms of the efficiency of the interaction of NP conjugated with the p18 peptide into both cancer and non-cancer cells of the human body.

Another objective of this work was to continue another experiment related to p28, and in this experiment, the impact that four different experimental conditions had at the level of the plasma membrane order in A549 cancer cells was evaluated. These four conditions were Free p28 (2.5 μM), Free p28 (50 μM), p28-NPs (250 μg/mL), which are called functionalized NPs (f-NPs), and NPs without p28 (250 μg/mL), which are called non-functionalized NPs (nf-NPs). This impact was assessed using a fluorescent probe called Laurdan (2-dimethylamino-6-lauroylnaphthalene) with a two-photon excitation microscopy.

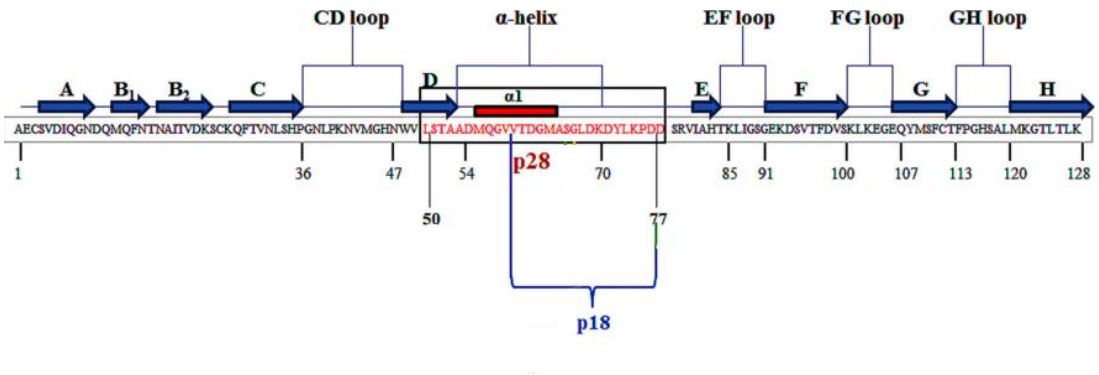


**Figure 7 -** Azurin's sequence (128 amino acids), in the black box is located the p28 peptide (28 amino acids) from amino acids 50-77, and from amino acids 60-77 it is located the p18 peptide. Source: Yaghoubi *et al.,* 2020 (doi: 10.3389/fonc.2020.01303).

# 3. Materials and Methods

## 3.1. Peptide synthesis

p18 with a cysteine in the C-terminal (CLSTAADMQGVVTDGMAS-$NH_2$, 1756.02 Da) was synthetized and provided by CASLO ApS., LTD. at 98.7% purity percentage.

p28 with a cysteine in the C-terminal (CLSTAADMQGVVTDGMASGLDKDYLKPDD-$NH_2$, 3017.29 Da) was synthetized and provided by CASLO ApS., LTD. At > 95% purity percentage.

## 3.2. Cell Culture and Growth Conditions

The A549 human lung cancer cell line, which was purchased from the European Collection of Authenticated Cell Cultures (ECACC), was used throughout this thesis. Cells were grown in Dulbecco's Modified Eagle Medium (DMEM; Gibco® by Life Technologies), supplemented with 10% heat-inactivated Fetal Bovine Serum (FBS; Gibco® by Life Technologies), 10,000 U/mL of penicillin, and 100 mg/mL of streptomycin (PenStrep, Invitrogen). These cells were chemically detached with 0.05% TrypLE™ Express (Gibco® by Life Technologies) and passed two to three times a week. The 16HBE14o- human bronchial non-cancer cell culture was used as a control cell line. It was cultured in Minimum Essential Medium (MEM) without Earls salts supplemented with 10% of FBS, 10000 U/mL penicillin, and 10000 mcg/mL streptomycin. This cell line was cultured in fibronectin-coated T-flasks.

Both cancer and non-cancer cells were maintained at 37 ºC in a humidified environment with 5% $CO_2$ (Binder CO2 incubator C150), to preserve the pH of the growth medium.

### 3.3. Conjugation of p18-C or p28-C Peptide to PLGA-PEG-Mal

The interaction between maleimide (Mal) and the thiol (SH) group present in the cysteine (C-terminal) of the peptide was promoted in order to conjugate p18 or p28 to PLGA-PEG-Mal. First, 15 mg of PLGA-PEG-Mal was dissolved in 1 mL of N,N-dimethylformamide (DMF, CARLO ERBA) for an hour under soft agitation, 1.5 mg of tris(2-carboxyethyl) phosphine hydrochloride (TCEP, Aldrich) was dissolved in 1 mL of DMF, and the peptide was also dissolved in 1 mL of DMF during 15 minutes. 150 µL of TCEP was added to the peptide solution after 15 minutes, and the mixture was then gently stirred for a further hour at room temperature. The TCEP + peptide combination was then combined with the volume of PLGA-PEG-Mal solution, and the mixture was then agitated at 4 °C for 24 hours.

The next day, the PLGA-PEG-Mal-peptide solution was precipitated two times with diethyl ether (Sigma-Aldrich®), 16 mL each time, and 3 times with ultrapure water (MilliQ station from Millipore Corporation), 5 mL each time, respectively. The water used is to dissolve the free peptide that precipitated with the polymer, and thus wash the pellet so that it is only constituted by the polymer PLGA-PEG-Mal-peptide. Following each precipitation, the pellet was sonicated (Ultrasonic Cleaner, Branson 200) for 3 minutes, centrifuged (Centrifuge 5840R, Eppendorf) for 5 minutes at 3300xg at 4 °C, and then the supernatant was collected and stored at -80 °C overnight. The pellet was lyophilized in a freeze dryer (ScanVac CoolSafe, LaboGene) the next day, and the amount of PLGA-PEG-Mal-peptide recovered was weighted. Lastly, the PLGA-PEG-Mal-peptide pellet was stored at -20 ℃.

### 3.4. Indirect Quantification by HPLC to Determine the Efficiency of PLGA-PEG-Mal-peptide Conjugation

The supernatants collected during the conjugation step were evaluated using a Hitachi LaChrom Elite® high-performance liquid chromatography (HPLC) System (Hitachi High Technologies America, Inc) to ascertain the percentage of conjugation of the peptide to PGLA-PEG-Mal. A LiChrospher® 100 RP-18 column (5 m, 4.6 x 250 mm) was used for the chromatographic separations, along with a LiChrospher 100 RP-18 guard column and stationary phase kept at 25 °C. Two acetonitrile buffers (2% CH3CN, Carlo Erba), 0.05% trifluoroacetic acid (TFA, Sigma), and ultrapure water made up the mobile phase. The detector was set at 220 nm and the HPLC equipment was configured for UV-Vis. Each sample was examined for 40 minutes while the flow rate was adjusted to 1 mL/min and the injection volume to 90 µL. A calibration curve for determining the peptides' concentration was performed under the same conditions (3, 6, 15, 45, 90, 125, 250, and 400 µg/mL dissolved in ultrapure water). To ensure that none of the reagents employed in the conjugation process interfered with the analysis, control samples DMF and TCEP were also run through the HPLC column used. To determine peptides' conjugation to the polymer, we determined how much of the peptide did not conjugate to the polymer using the supernatants of diethyl ether and ultrapure water precipitation steps. Finally, the EZChrom Elite software was utilized to calculate the area under the

curve of each peak. To determine the peptide concentration at each sample from the precipitation steps, an equation for the calibration curve was first determined (Equation 1):

$$Area\ (Au) = a\ \times peptide\ concentration\ + b$$

(Equation 1)

After calculating the concentration of the peptide present in each supernatant, the final mass of the peptide ($m_{f\ peptide}$) was calculated to determine the conjugation efficiency percentage (CE%) with the value of the initial mass of the peptide ($m_{i\ peptide}$):

$$Conjugation\ Efficiency\ (CE;\ \%) = \left(\frac{mi\ peptide - mf\ peptide}{mi\ peptide}\right) \times 100$$

(Equation 2)

### 3.5. Production of PLGA Nanoparticles by Nanoprecipitation Method

Two types of NPs were made: non-functionalized NPs and functionalized NPs. The non-functionalized NPs do not have p18 or p28 exposed in their surface while functionalized NPs do. To produce non-functionalized NPs, 20 % PLGA-PEG-Mal, 10 % PLGA-FKR648 (fluorescent probe, only for cellular interaction), and 70 % (for cellular interaction) or 80% (for membrane order experiments) PLGA (50:50 LA:GA; 44 kDa, Purasorb® PDLG 5004A, Corbion) were combined, to a total of 20 mg of polymer. The same was used to produce functionalized NPs but instead of using PLGA-PEG-Mal, PLGA-PEG-Mal-p18C or PLGA-PEG-Mal-p28C were used. In each formulation, 3 mL of DMF (organic phase) were added to the polymers and left at room temperature overnight to a complete dissolution. In the next day, using a needle in a previously cut 1000 µL tip, the organic phase was slowly and steadily added into the aqueous phase containing 10 mL of Tween 80 1 % at pH 7.4 and each solution was kept under soft agitation for 3 hours to evaporate the organic solvent. After the NPs production, the washing step was carried out to remove the surfactant and elute the organic solvent that had not evaporated yet. This process was proceeded by using Amicon Ultra-15 Centrifugal Filter units (100 kDa) (Merk Millipore, UFC910024) and cleaned with ultrapure water combined with centrifugation at 600xg, 4 ℃, for 10 minutes. Lastly, the NPs colloidal solutions were collected into a microtube and stored at 4 ℃ until characterization through Zetasizer.

### 3.6. Characterization of Nanoparticles Using Zetasizer Software

The NPs were characterized by using the software Zetasizer which analyzes their average size (Z-average), polydispersity index (PDI) by dynamic light scattering (DLS) (0-1), and zeta-potential (ζ-potential) through Laser Doppler Anemometry (LDA), using a Malvern Zetasizer Nano ZS

instrument (Malvern Instruments Ltd., Worcestershire, UK). Each sample (before and after the washing step) was diluted (1:100, v/v) with 10 mM NaCl pH 7.4, and the laser was set to a wavelength of 633 nm and left for stabilization for 20 minutes.

### 3.7. Cell-p18C Nanoparticles Interaction by Flow Cytometry

First, the preparation of the cell lines A549 lung cancer cells and 16HBE14o- human bronchial non-cancer cells was carried out to compare the cell uptake of the functionalized NPs and non-functionalized NPs. In total, eight 6-well plates were used, four for each cell line (one treated with functionalized NPs and the other with non-functionalized NPs with acid wash, the other two were without the acid wash). A 6-well plate is intended to have $5x10^5$ cells/well for the A549 lineage and $1x10^6$ cell/well for the 16HBE14o- lineage. All plates were put at 37 ℃ in an incubator overnight. On the following day, the treatment of functionalized and non-functionalized NPs was carried out in which the cells were washed with PBS 1x and treated with different concentrations of functionalized NPs and non-functionalized NPs (50, 100, 250, 500 µg/mL) with and without the acid wash.

The wells were incubated for 4 hours, after which the cells were washed with phosphate buffer saline (PBS) twice and two 6-wells of each lineage (four 6-wells in total) were acid washed with a buffer composed of 0.5 M NaCl, 0.2 M acetic acid at pH 3 (dissolved in MilliQ Water). Then, cells were detached using TrypLE™ Express before being incubated for 2 minutes. After this time, 1 mL of medium was placed in each well to neutralize the effect of the TrypLE™. Then, the contents of each well were transferred into 15 mL Falcon tubes and centrifuged for 3 minutes at 1200 rpm. The supernatant was collected and 1 mL of paraformaldehyde (PFA) 2 % in PBS was added to each tube, the samples were incubated at room temperature for 30 minutes and centrifuged again at 1200 rpm for 3 minutes to remove excess PFA. The pellet was resuspended in 1 mL of PBS after the supernatant was removed, the tubes were centrifuged again, and the pellet was resuspended in 350 µL of PBS. The cells were then examined by Flow Cytometry (BD – Accuri C6 Plus). To analyze the data obtained by the Flow Cytometer the FlowJo™ software was utilized, where it was calculated the geometric mean fluorescence intensity (GEO MFI) values of each treatment, which is the parameter used to evaluate the interaction the NPs had with the cells.

### 3.8. Detection of Variations on the Plasma Membrane in A549 Cells Using Laurdan and Two-Photon Excitation Microscopy

For this experiment, both f-NPs with p28 and nf-NPs were produced and characterized as described above, after making sure that both types of NPs were suitable for use, A549 cells were seeded on µ-Slide 8 well IBIDI glass bottom chambers (ibidi®) with $7.5x10^5$ cells and left to adhere and grow overnight in a $CO_2$ incubator (5 %) at 37 ℃. On the next day, the medium was collected, and the cells were incubated with Free p28 (2.5 µM and 50 µM), f-NPs (250 µg/mL), and nf-NPs (250 µg/mL). For control, the cells were incubated only with the medium. Cells were left for 4 h before 5 µM of the

fluorescent dye Laurdan was added and the cells were incubated in a $CO_2$ incubator at 37 ℃ for 20 minutes. The experiments were analyzed on an inverted microscope (model no. DMI6000) of Leica TCS SP5 (Leica Microsystems CMS GmbH, Mannheim, Germany) with a 63x water (1.2-numerical-aperture) apochromatic objective. The data from the two-photon excitation microscopy was obtained with a Ti:sapphire laser (Mai Tai, Spectra-Physics, Darmstadt, Germany) as the excitation light source. The excitation wavelength was set to 780 nm and the fluorescence emission was collected at 400-460 nm and 470-530 nm to calculate the generalized polarization (GP) images. Laurdan GP images were analyzed through a homemade software called GPIMAGE based on a MATLAB (MathWorks) environment, with the GP value defined as:

$$GP = \frac{I_{400-460} - GI_{470-530}}{I_{400-460} + GI_{470-530}}$$

(Equation 3)

Where G is the calibration factor for the experimental setup, which is obtained from imaging Laurdan in dimethyl sulfoxide (DMSO) using the same experimental conditions as those set for the measurement in living cells [126]. At least 5 to 10 independent cells were analyzed per condition. The dark counts were subtracted from all intensity values and, in the analysis, only Regions of Interest (ROI) corresponding to the plasma membranes in each cell were selected, restricting, therefore, the analysis to this cellular component.

# 4. Results and Discussion

## 4.1. Interaction of p18 Peptide-functionalized Polymeric Nanoparticles with A549 and 16HBE14o- Cells

### 4.1.1. Conjugation Efficiency of p18-C to PLGA-PEG-Mal Polymer Using HPLC

Initially, the procedure consisted of promoting the Maleimide-Thiol click chemistry between maleimide and the thiol (SH) group present on the cysteine of p18. A cysteine was added to the C-terminal of the p18 sequence, the hydrophilic domain, for the same reason it was added to the p28 sequence in the experiences made by Garizo *et al.* [117], because the natural sequence of this peptide does not have a cysteine amino acid residue. So, binding the p18 cysteine with maleimide enhances the exposure of the peptide's hydrophobic domain towards the cells, while the hydrophilic domain becomes less exposed because it is attached to PLGA-PEG-Mal. After conjugating p18 with PLGA-PEG-Mal, this conjugate was cleaned by diethyl ether and ultrapure water to remove all the reagents used in the conjugation process, and the p18 that did not bind to the polymer.

Through HPLC, it was possible to quantify the p18 that did not bind to PLGA-PEG-Mal, and the eight reference samples with specific concentrations of p18 were analyzed to identify the location

of the peaks related to the peptide, which allowed to identify and quantify the area of the p18 peaks detected in the PLGA-PEG-Mal-p18C supernatants. As control samples, it was used the reagents from the conjugation process. As a result, HPLC spectrums were obtained and evaluated by noting the retention times of all the peaks and measuring the area of the ones that were from p18 (Table 6).

**Table 6 -** List of all samples analyzed by high-performance liquid chromatography (HPLC) with the respective retention time of the identified peaks. Reagents, p18 that did not conjugate to PLGA-PEG-Mal, and p18 reference samples.

| **Sample** | | **Retention time (min)** | **Area (Au) p18 peaks** |
|---|---|---|---|
| **Reagents** | $H_2O$ | 2.36; 2.76 | - |
| | Diethyl ether | 2.18; 2.42; 2.59; 2.79; 6.88; 25.94; 28.11 | - |
| | DMF | 3.3 | - |
| | TCEP | 14.20; 19.52; 20.58 | - |
| **PLGA-PEG-Mal-p18C (p18 that did not conjugate)** | $1^{st}$ sup – ether | - | - |
| | $2^{nd}$ sup – ether | - | - |
| | $3^{rd}$ sup – $H_2O$ | 9.14; 11.28; 12.3 | 925186 |
| | $4^{th}$ sup – $H_2O$ | 9.16; 11.3; 12.3 | 252436 |
| | $5^{th}$ sup – $H_2O$ | 9.14; 11.32; 12.31 | 54925 |
| **p18 (µg/mL)** | 3 | 10.5 | 9865 |
| | 6 | 9.12; 11.28 | 23460 |
| | 15 | 9.07; 11.27 | 73957 |
| | 45 | 9.12; 9.56; 10.03; 11.29 | 315467 |
| | 90 | 7.86; 9.12; 9.58; 10.07; 11.29; 11.64 | 977663 |
| | 125 | 7.86; 9.13; 9.58; 10.08; 11.29; 11.63 | 1345363 |

| | | | |
|---|---|---|---|
| | 250 | 7.82; 9.10; 9.56; 10.07; 11.27; 11.63 | 2671394 |
| | 400 | 7.84; 9.10; 9.56; 10.06; 11.29; 11.63; 12.46; 14.68; 16.96 | 4252117 |

The area of the peaks of the p18 reference samples is proportional to the concentration of p18, therefore, a graph was produced that allowed to obtain an equation that permits the calculation of the free p18 mass detected on the PLGA-PEG-Mal-p18 supernatants (Figure 8 and Table 7).

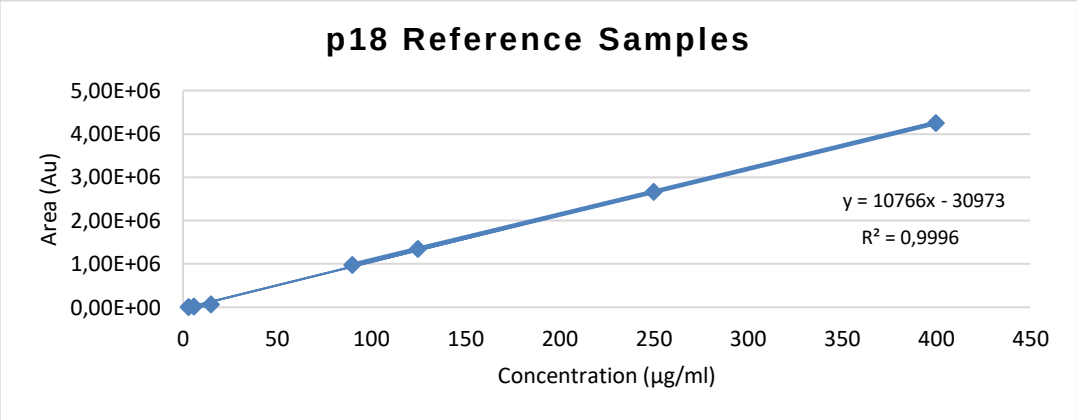


$$Area\ (Au) = 10766 \times [\text{p18}]\ (\mu g/mL) - 30973$$

**Figure 8 -** Linear regression produced from the p18 reference sample values (Table 6), combined with the linear equation that allowed to calculate the p18 concentration through the area of the p18 peaks detected on the PLGA-PEG-Mal supernatants (Table 7). Note: the peak area value of the 45 µg/mL sample was considered an outlier

**Table 7 -** Calculated mass of free p18 detected on the PLGA-PEG-Mal-p18 supernatant spectrums by using the area of the p18 peaks detected (Table 6), combined with the equation produced from the p18 reference samples (Figure 8). From the initial p18 mass (2 mg), it was lost a total of 0.609 mg of p18, which turned the conjugation efficiency to 69%.

| PLGA-PEG-Mal-p18 | [p18] (µg/mL) | p18 (mg) |
|---|---|---|
| **1st sup – ether** | - | - |
| **2nd sup – ether** | - | - |
| **3rd sup – $H_2O$** | 88,81603593 | 0,44408018 |
| **4th sup – $H_2O$** | 26,32541198 | 0,13162706 |

| | | |
|---|---|---|
| **5th sup – $H_2O$** | 7,978945045 | 0,039894725 |

The peaks related with p18, from the p18 reference samples results (Table 6), had a retention time of 7.84; 9.10; 9.56; 10.06; 11.29; 11.63; 12.46; 14.68; 16.96 minutes. Diethyl ether was used to precipitate PLGA-PEG-Mal-p18 and to precipitate free p18, and it also removed the other reagents, which is the reason why no peak related to the peptide was seen on the first two supernatants (corresponding to ether). Although, after adding ultrapure water several times (3rd, 4th, and 5th supernatant), it is expected to see peaks related to free p18 because this peptide is water-soluble, so if it is not conjugated to PLGA-PEG-Mal, it dissolves and stays in solution. Furthermore, because PLGA-PEG-Mal is not water soluble, p18 remains precipitated if it is bound to this polymer. Therefore, we know that the peaks with the retention time of approximately 9.14, 11.30, and 12.31 minutes, corresponding to p18, did not bind to the polymer because it appears on the ultrapure water supernatants (Table 6), which means that these peaks are free p18. After calculating the final mass of p18 (Table 7), it was concluded that 0,609 mg, out of the initial 2 mg used, corresponds to the mass of p18 that did not bind in the conjugation process, making the conjugation efficiency of 69%. Meaning that almost 1.4 mg of p18 was bound to PLGA-PEG-Mal polymer. In conclusion, the final conjugation product can be used to produce PLGA-PEG-Mal NPs functionalized with p18 to evaluate the p18-NPs interaction with the cells.

### 4.1.2. Characterization of PLGA-NPs

After the production of PLGA-NPs by the nanoprecipitation method we obtained two samples, functionalized NPs and non-functionalized NPs. These samples were characterized to evaluate their physicochemical characteristics, such as the Z-average, ζ-potential and PDI values. In ζ-potential measurements, an electrical field is applied across the sample and the movement of the NPs is measured by laser doppler velocimetry (LDV). NPs with a ζ-potential between -10 and +10 mV are considered neutral, while NPs with ζ-potential bigger than +30 mV or lesser than -30 mV are strongly cationic or strongly anionic, respectively. The ζ -potential can influence an NP's propensity to cross the membrane, with cationic particles typically displaying greater toxicity due to rupture of the cell wall [127]. The PDI value is a measure of how well the NPs manage the size distribution. The range of the particle distribution index, or PDI, is 0.0 (completely uniform sample) to 1.0 (highly polydisperse sample with multiple particle size populations). Values of 0.2 and lower are typically regarded as acceptable in practice for polymer-based NP materials, whereas values larger than 0.7 show that the sample has an extremely wide range of particle sizes and is most likely not suitable for DLS analysis [128]. Table 8 shows the characterization we were able to achieve using our two samples, and the results are presented as the average of 3 measurements.

**Table 8 -** Physicochemical characterization of fluorescent p18-functionalized and non-functionalized NPs produced by the nanoprecipitation method before and after the washing step. The results are presented as the average of 3 measurements.

| Type of Nanoparticles | | Z-average (nm) | PDI | ζ-potential (mV) |
|---|---|---|---|---|
| **Non-functionalized** | After washes | 127.8 | 0.09 | -9.99 |
| **Functionalized** | After washes | 116.5 | 0.13 | -10.08 |

We can observe that the ζ-potential in both types of NPs is similar and considered neutral (-9.99 mV and -10.08 mV for nf- and f-NPs), the PDI value of the f-NP (0.13) is bigger than the nf-NPs (0.09) which means that this population was more heterogeneous, and that is mostly caused by NP aggregation. Lastly, the Z-average values are approximately 100 nm which is the optimal size for cell uptake by mammalian cells, nf-NPs had a Z-average of 127.8 nm and f-NPs of 116.5 nm. In conclusion, both types of NPs are appropriate for being tested on cells to compare the cell interaction of non-functionalized NPs and functionalized NPs in cancer and normal cells by using Flow Cytometry.

### 4.1.3. Characterization of PLGA-PEG-Mal-p18C NPs by Flow Cytometry

In this work, both A549 human lung cancer and 16HBE14o- human bronchial non-cancer cells were incubated with different concentrations of fluorescent p18-functionalized NPs and non-functionalized NPs (50, 100, 250, and 500 µg/mL). By analyzing the samples by flow cytometry, the fluorescent intensity is detected by the FL4 detector, and it is possible to obtain a histogram that exhibits the fluorescence intensity associated with the cells, an example of that is in Figure 9. After obtaining the fluorescence intensity values, the Geo MFI values of each treatment with f- or nf-NPs were calculated with the FlowJo™ software to verify which type of NP interacted more with the cells.

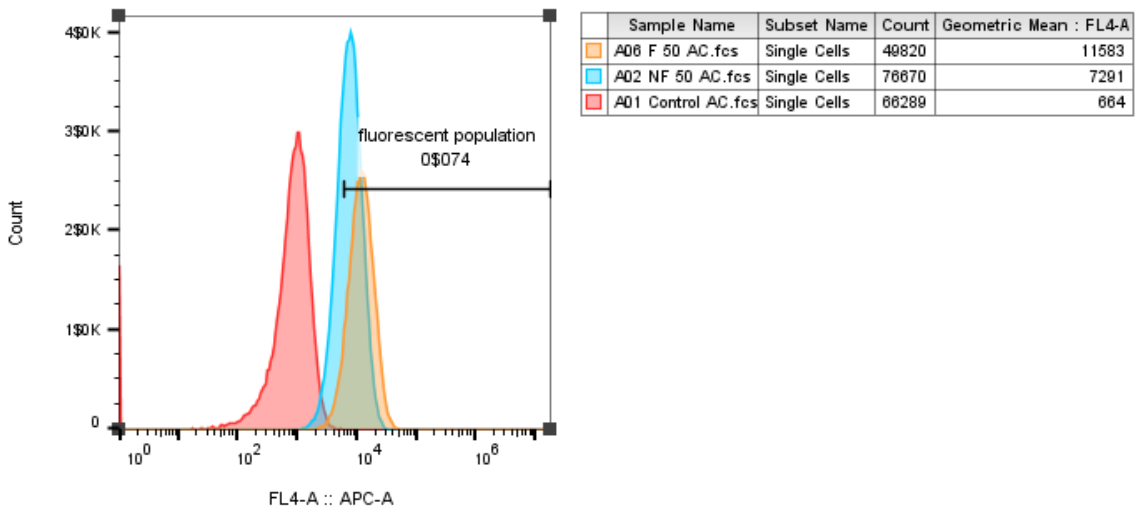


| | Sample Name | Subset Name | Count | Geometric Mean : FL4-A |
|---|---|---|---|---|
| | A06 F 50 AC.fcs | Single Cells | 49820 | 11583 |
| | A02 NF 50 AC.fcs | Single Cells | 76670 | 7291 |
| | A01 Control AC.fcs | Single Cells | 66289 | 664 |

**Figure 9** - Histogram produced from the fluorescence values (FL4.A :: APC-A) with the number of A549 cells (count) incubated with 50 µg/mL of p18-functionalized NPs (F) and non-functionalized NPs (NF), both with acid wash (AC). Both samples are evaluated against a control.

To see if there is indeed an advantage in using a smaller peptide, we compared the results of the flow cytometry of p18 to the results made by Garizo *et al*.[117] of p28. Starting with the interaction between the cell line A549 and the NPs with or without the acid wash (Figure 10A and 10B) we can observe that p18-NPs (f-NPs) had more interaction with the cells than the nf-NPs in every concentration, which means that p18, just like p28, enhances the interaction of NPs with cells. However, p28-NPs had more interaction with the cells than p18-NPs in almost every concentration, with an exception on the interaction with acid wash in the concentrations 100 and 250 µg/mL, although not very significant. The identical happens with the interaction between the cell line 16HBE14o- and NPs with or without the acid wash. Once more, p18-NPs had more interaction than nf-NPs, but p28-NPs still had more interaction to the cells than p18-NPs (Figure 10C and 10D), which in this case it can be a good thing because we do not want NPs conjugated with CPPs entering the non-cancer human cells.

In Figure 11, it is possible to compare the Geo MFI of the two cell lines under study interacting with NPs conjugated with p18 (Figure 11A) and, just like it happened with studies made with p28 (Figure 11B), NPs conjugated with p18 are also cancer cell-specific because we can observe more interactions with the cancer cell line than the non-cancer one. However, as previously seen, p18-NPs were not more efficient than p28-NPs in interacting with the cells under study, which makes this peptide, in general, less advantageous, so, proceeding with new experiments with p18 that have already been done with p28 does not seem reasonable.

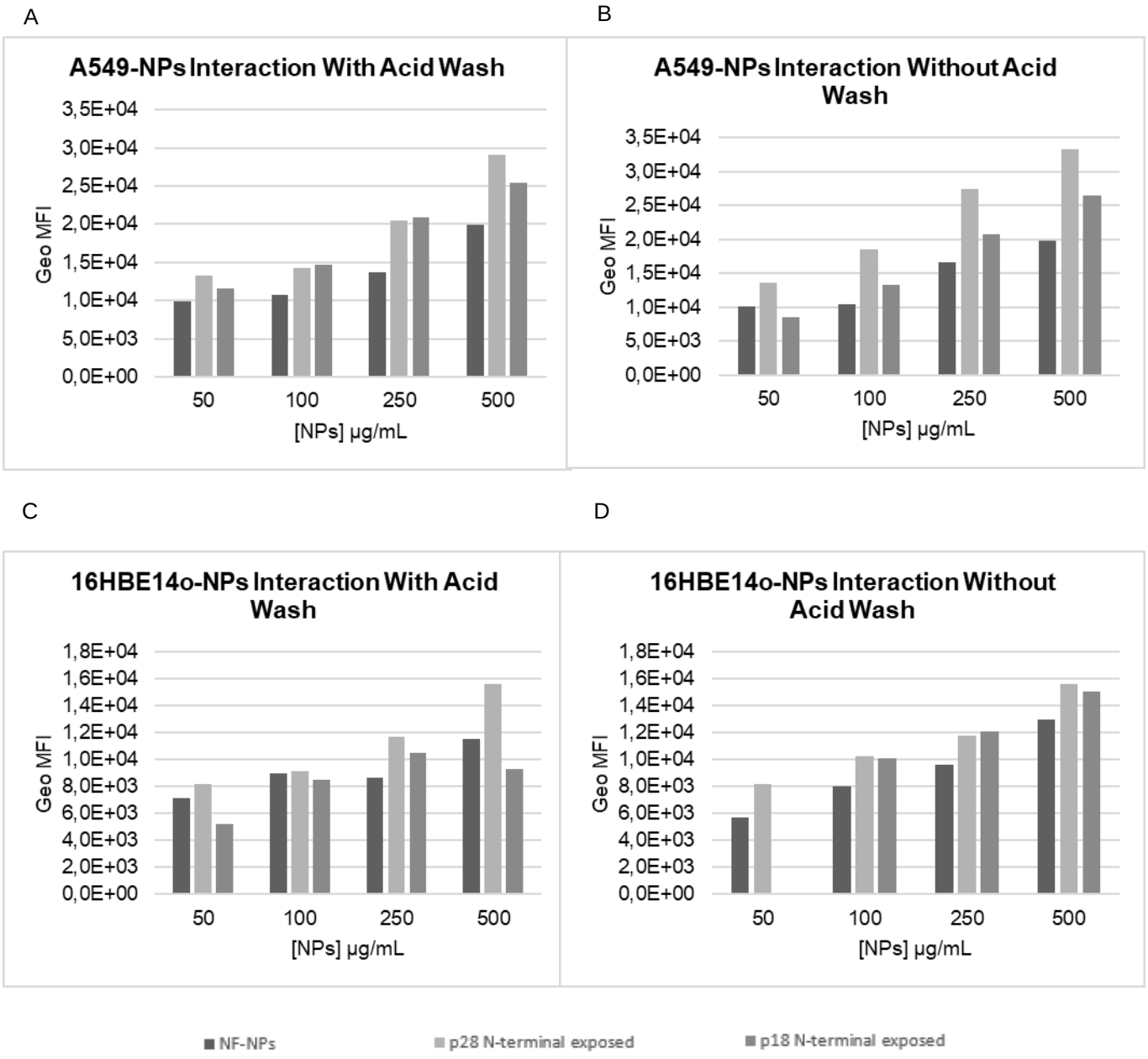


**Figure 10 -** (A) Comparison of Geo MFI values of A549 cells incubated with non-functionalized NPs and NPs functionalized with p18 and p28, with acid wash. (B) Comparison of Geo MFI values of A549 cells incubated with non-functionalized NPs and NPs functionalized with p18 and p28, without acid wash. (C) Comparison of Geo MFI values of 16HBE14o- cells incubated with non-functionalized NPs and NPs functionalized with p18 and p28, with acid wash. (D) Comparison of Geo MFI values of 16HBE14o- cells incubated with non-functionalized NPs and NPs functionalized with p18 and p28, without acid wash.

A B

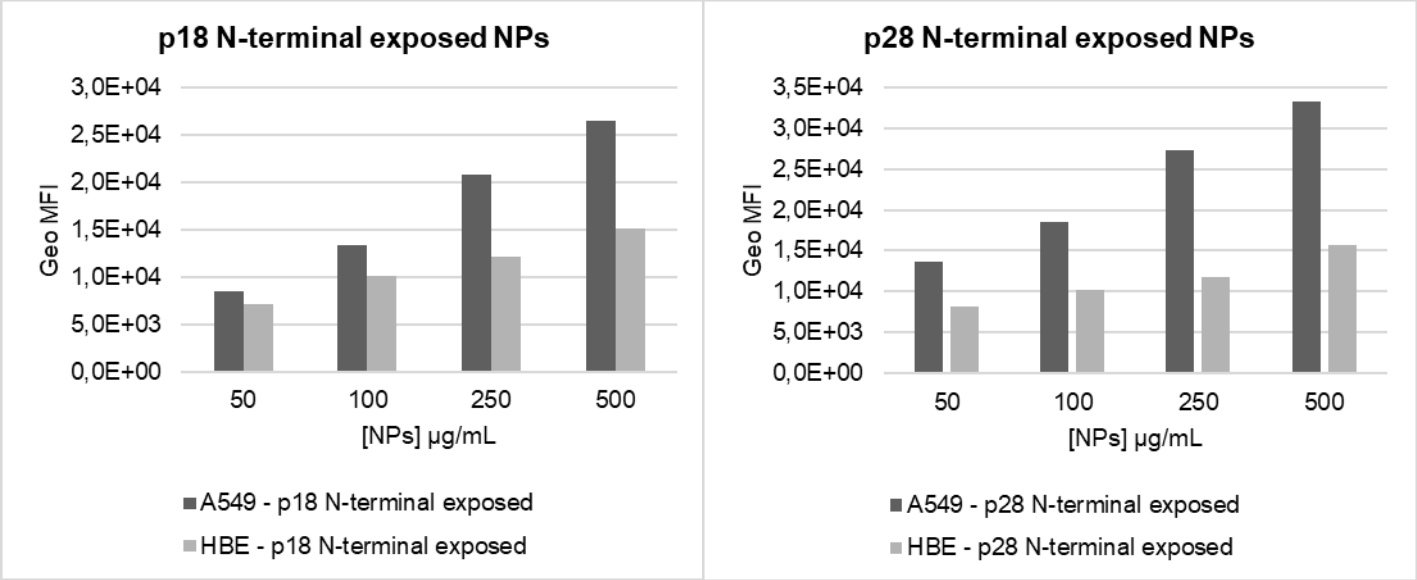


**Figure 11 -** (A) Comparison of Geo MFI values of A549 and 16HBE14o- cells incubated with functionalized NPs with peptide p18. (B) Comparison of Geo MFI values of A549 and 16HBE14o- cells incubated with functionalized NPs with peptide p28.

## 4.2. Detection of Variations on the Plasma Membrane in Cells using p28-NPs Nanosystems

### 4.2.1. Evaluation of the Plasma Membrane Integrity in A549 Cells

It has already been observed that azurin protein and its peptide p28 leads to a decrease content of lipid raft components GM-1 and CAV1 [129]. Lipid rafts are present in the outer leaflet of the membranes and contains the combinations of specific lipids, cholesterol, and sphingolipids, forming highly condensed ordered membrane nanodomains. Their assembly occurs very quickly through van der Waals forces and hydrogen bonds between the $OH^-$ group of cholesterol and the sphingolipids [129,130]. Evidence shows that changes in cholesterol metabolism is involved in carcinogenesis, since increased cholesterol levels are associated with a higher cancer incidence. Therefore, molecules that help reduce these high levels are beneficial because they reduce the risk and mortality of some cancers [131]. The membranes, composed of sphingolipids, cholesterol and glycerophospholipids, exhibit two coexisting fluid phases: the liquid-ordered membrane phase and the liquid-disordered membrane phase. Because loosely packed membranes are more polar due to increased water molecule penetration into the lipid bilayer, packing order can be used to gauge membrane order. By using fluorescent membrane probes whose emission spectra are solvent-polarity dependent and can provide information on membrane order, this shift in polarity can be used to evaluate the degree of condensation of membranes [132].

Having this in mind, the effects of four different treatments were evaluated, such as Free p28

(2.5 μM and 50 μM), f-NPs (250 μg/mL), and nf-NPs (250 μg/mL), in the organization of the plasma membrane in A549 cancer cells, by assessing the membrane fluidity with the fluorescent probe Laurdan.

Due to dipolar relaxation processes that take place close to the Laurdan molecule (Figure 12), this probe is extremely sensitive to the physical condition of the membranes. This phenomenon occurs in membranes because of the water molecules in the bilayer that are situated between the interface and the lipid chains. A decrease in the excited state energy and subsequent red-shift of the Laurdan emission maxima result from the fluid membrane's enhanced hydration and the potential for water molecules to reorient along the probe excited-state dipole. In contrast, the rate of relaxation and hydration are both low in gel phase membranes, leading to a minimal emission spectrum shift. Laurdan exhibits a blue shift in emission with increasing membrane condensation caused by an alteration in the dipole moment of the probe as a consequence of exclusion of water molecules from the lipid bilayer [133].

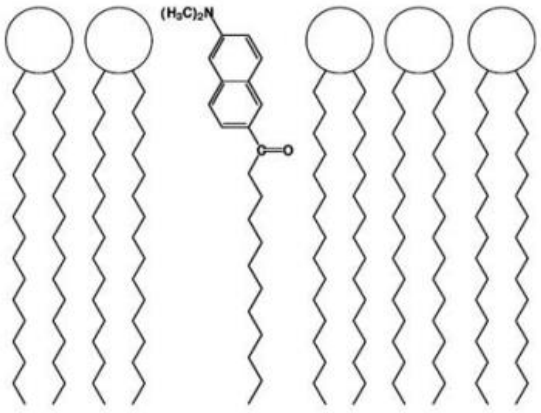


**Figure 12** – Structure of Laurdan and its orientation in the phospholipid layer. Source: Gaus *et al.,* 2006 (Doi: 10.1080/09687860500466857).

So, in this experiment the GP of Laurdan was measured in the coacervate droplets to evaluate the lipid membrane hydration, because GP measures surface hydration of lipid membranes [134]. GP values can state modifications in the biophysical properties of cell membranes caused by cellular adaptation to the culture conditions, such as media composition, which is the case of this experiment. Higher GP values are associated to higher membrane order and a less fluid membrane. The determination of GP values using Laurdan in fluorescence microscopy studies is one of the most widely-used methods to investigate changes in membrane fluidity.[135]

Firstly, for this experiment, p28 was bound to PLGA-PEG-Mal the same way it is described above on point 4.1.1. Conjugation Efficiency of p28-C to PLGA-PEG-Mal Polymer Using HPLC, which gave a conjugation efficiency of 78%. Then, the f-NPs and nf-NPs were produced by the nanoprecipitation method, but in this case without the fluorescent probe PLGA-FKR648. Their physicochemical proprieties were analyzed through DLS, and it was concluded that these NPs are

suitable for experimentation. After incubating the A549 cells with the four different experimental conditions for 4 hours, the fluorescent dye Laurdan was incubated for 20 min, and then these cells were analyzed on an inverted microscope.

Numerous pictures were taken to estimate the Laurdan GP values (Figure 13), and Laurdan fluorescence spectrum changes in the plasma membrane were quantified using the GP function as indicated in the Materials and Methods section. In each GP image, regions of interest (ROI) corresponding to the plasma membrane of cells were selected in such a way that values of the total membrane regions of a cell were obtained. These values were averaged to obtain a GP value for a single cell. The results are presented as the average of at least 5-10 cells per each condition. As it can be observed in Figure 14, every condition tested caused a decrease in the GP values measured in the plasma membrane order when compared with the control.

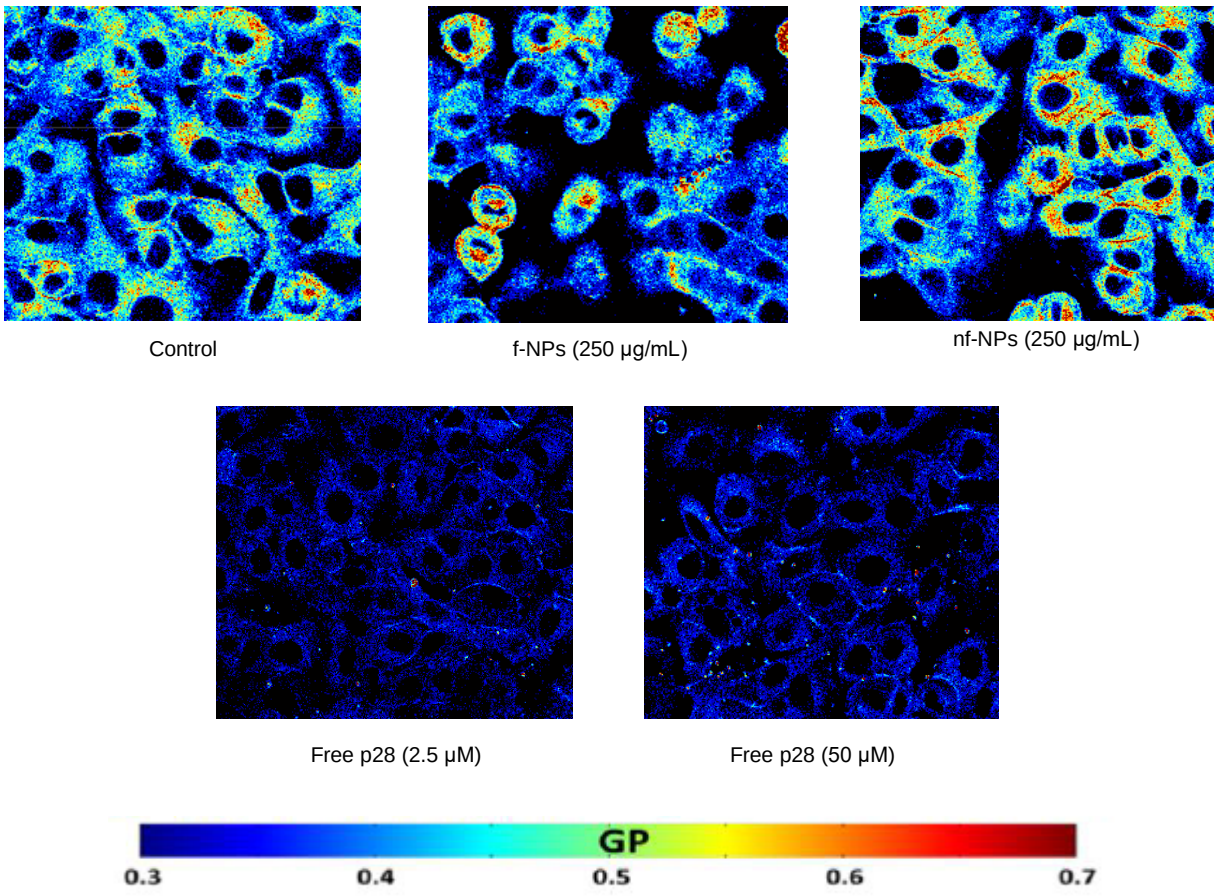


**Figure 13 –** Cells were incubated with DMEM without FBS containing 5 µM of Laurdan for 20 minutes at 37°C, 5% $CO_2$, after incubation with functionalized NPs (f-NPs) and non-functionalized NPs (nf-NPs) at 250 µg/mL, and free p28 peptide at 2.5 µM and 50 µM. Representative Laurdan GP images are shown.

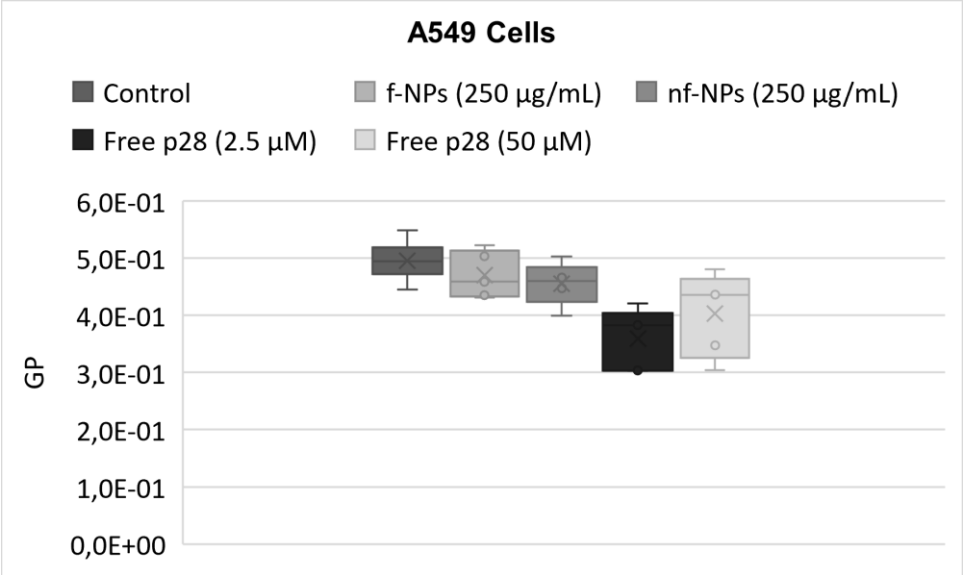


**Figure 14** – Average GP values obtained for cells after incubation with functionalized NPs (f-NPs) and non-functionalized NPs (nf-NPs) at 250 µg/mL, and free p28 peptide at 2.5 µM and 50 µM are shown for the plasma membrane of A549 human cancer cell line. Every experiment causes a decrease in the average GP value, after 4 hours, when compared with the control. Average GP values are expressed as mean ± SD from at least 5 to 10 individual cells in each condition.

The results show that the fluidity of the plasma membrane increases after exposure to the treatments, as evaluated by changes in the Laurdan GP values. However, these results need to be interpreted cautiously as the method used is not very accurate and precise when used in such a small scale. Therefore, in order to have more confidence in the results, it would be essential to perform this methodology more times for a good evaluation and interpretation. Nevertheless, from our preliminary data it is possible to observe in Figure 13 that the treatments which induced more fluidity of the plasma membrane are the ones with free p28 peptide. The peptide with the lowest concentration (2.5 µM) seems to have caused most disturbances in membrane organization than the treatment with a higher concentration (50 µM). One reason for this outcome could be that, as has been documented previously in the literature, at higher peptide concentrations, uptake is caused by a mechanism that starts from spatially constrained locations of the plasma membrane and causes a rapid distribution of the peptides throughout the cytoplasm. Previous observations noted an absence of endocytic vesicles when cells are treated with higher concentrations of CPPs, suggesting an uptake mechanism independent of endocytosis. While in lower concentrations, endocytosis predominates [56,136]. Therefore, higher concentrations of the peptide may have less of an impact on the plasma membrane since they do not enter cells through endocytosis. However, more replicates of this procedure would be necessary to validate this hypothesis. Regarding the treatments with NPs, the nf-NPs treatment caused more disruption to the plasma membrane than the f-NPs, although not very marked, which was not an expected result since the f-NPs are functionalized with p28. Therefore, it would be more

expected for the latter to have caused a greater fluidity to the membrane, however, since no big differences can be observed in Figure 13, once again, more experiments would be needed.

The reason why these 4 conditions have caused changes in the fluidity of the membrane of A549 cells (Figure 14) may be that the entry of free p28 and p28-NPs is preferentially through caveolae/lipid rafts. Therefore, they most likely displaced Cav-1 from the membrane, at least temporarily, which disrupted the raft organization, likely affecting plasma membrane organization and reducing the proportion of liquid-ordered membrane/domains. These findings are consistent with earlier findings from our group's studies, with the exception that in these studies azurin protein was utilized. The studies showed that azurin causes biophysical changes at the plasma membrane level, which may attenuate signaling pathways involved in motility, adhesion, and invasiveness [130].

# 5. Conclusion

Nanotechnology has been intensively studied in the past years showing a huge potential for cancer therapy, especially due to the NPs used that are around the nanometer scale, which is a size scale adequate to enter living human cells. The NPs most commonly used are liposomes, polymeric nanoparticles, dendrimers, quantum dots, and carbon nanotubes. NPs, when utilized as drug delivery molecules, have shown promise to increase the efficacy and safety of cancer therapies, however, improved delivery and a more specific targeting to cancer cells is needed. A way to obtain this is by functionalizing NPs with targeting ligands displayed at their surface, such as CPPs.

The first objective of this current work was a follow up of the work previously made by our group [117], with a minor modification to the CPP that utilized p18 rather than the complete p28 peptide sequence. The size and lack of the domain in charge of the cytotoxicity activity present in C-terminal are the only differences. By introducing a cysteine to the peptide's C-terminal, which enabled conjugation with PLGA-PEG-Mal through the maleimide-thiol click reaction while leaving the N-terminal exposed and open to interactions, the hydrophobic domain of p18 was thus investigated. By using HPLC to analyze the PLGA-PEG-Mal-p18 supernatants, the conjugation efficiency of this reaction was determined to be 69%, indicating that it was successfully carried out and that p18 could bind to PLGA-PEG-Mal. After that, p18-functionalized and non-functionalized PLGA-NPs with known properties were formulated and exposed to cells for a flow cytometry analysis. The results from flow cytometry were compared to previous data of p28-functionalized NPs and indicate that p18-NPs and p28-NPs both have a higher specificity to lung cancer cells than bronchial non-cancer cells. However, p18 did not demonstrate a higher specificity to cells than p28; it does, however, seem to be a slight advantage of interacting less with the 16HBE14o- cell line. However, overall, this peptide did not demonstrate advantages in terms of interacting more with the A549 human cancer cell line, thus it will not be used for now in upcoming work.

For the second objective of this thesis p28 was conjugated to PLGA-PEG-Mal in the same manner as p18, with a conjugation efficiency of 78%. After that, PLGA-NPs with and without p28

functionalization were created, and DLS confirmed they have the physicochemical properties needed for future testing. In order to identify the possible effects at the plasma membrane using the fluorescent dye Laurdan, both types of NPs were incubated with A549 cancer cells, as well as the free unconjugated p28 (2.5 μM and 50 μM). It has already been noted that the azurin protein and its peptide, p28, can lower the levels of the lipid raft components GM-1 and CAV1, increase membrane fluidity, and encourage endocytosis [129]. The same observations were made in this work. In all four experimental conditions used here, a decrease in the membrane order was observed, with free p28 at the lowest concentration showing the most significant effect. In addition, both non-functionalized and functionalized NPs exhibited the same behavior, however, no differences were observed regarding the presence of p28 at the surface of the NPs. It may be that, although cells may uptake NPs by endocytosis which induces the differences observed related to the control, the levels of p28 present in there may not be enough for the changes to be observed by this technique. So, in conclusion, this suggests that targeting cancer cells by acting at the membrane level may be a novel approach, opening up the possibility of developing novel treatment approaches and drug delivery systems based on their activities, which may improve the absorption and efficiency of other medications.

# 6. References


1. Zhao CY, Cheng R, Yang Z, Tian ZM. Nanotechnology for Cancer Therapy Based on Chemotherapy. *Molecules*. 2018;23(4):826. doi:10.3390/molecules23040826

2. Saini R, Saini S, Sharma S. Nanotechnology: The future medicine. *J Cutan Aesthet Surg*. 2010;3(1):32. doi:10.4103/0974-2077.63301

3. Bayford R, Rademacher T, Roitt I, Wang SX. Emerging applications of nanotechnology for diagnosis and therapy of disease: a review. *Physiol Meas*. 2017;38(8):R183-R203. doi:10.1088/1361-6579/aa7182

4. Kumar R, Mondal K, Panda PK, et al. Core–shell nanostructures: perspectives towards drug delivery applications. *J Mater Chem B*. 2020;8(39):8992-9027. doi:10.1039/D0TB01559H

5. Saxena SK, Khurana SMP, eds. *NanoBioMedicine*. Springer Singapore; 2020. doi:10.1007/978-981-32-9898-9

6. Khan I, Saeed K, Khan I. Nanoparticles: Properties, applications and toxicities. *Arabian Journal of Chemistry*. 2019;12(7):908-931. doi:10.1016/j.arabjc.2017.05.011

7. Grodzinski P, Kircher M, Goldberg M, Gabizon A. Integrating Nanotechnology into Cancer Care. *ACS Nano*. 2019;13(7):7370-7376. doi:10.1021/acsnano.9b04266

8. Heinz H, Pramanik C, Heinz O, et al. Nanoparticle decoration with surfactants: Molecular interactions, assembly, and applications. *Surface Science Reports*. 2017;72(1):1-58. doi:10.1016/j.surfrep.2017.02.001

9. Jin C, Wang K, Oppong-Gyebi A, Hu J. Application of Nanotechnology in Cancer Diagnosis and Therapy - A Mini-Review. *Int J Med Sci*. 2020;17(18):2964-2973. doi:10.7150/ijms.49801

10. Ghasemi Y, Peymani P, Afifi S. Quantum dot: magic nanoparticle for imaging, detection and targeting. 2009;80(2):156-165.

11. Reshma VG, Mohanan PV. Quantum dots: Applications and safety consequences. *Journal of Luminescence*. 2019;205:287-298. doi:10.1016/j.jlumin.2018.09.015

12. Xiang QM, Wang LW, Yuan JP, Chen JM, Yang F, Li Y. Quantum dot-based multispectral fluorescent imaging to quantitatively study co-expressions of Ki67 and HER2 in breast cancer. *Experimental and Molecular Pathology*. 2015;99(1):133-138. doi:10.1016/j.yexmp.2015.06.013

13. Loo C, Lin A, Hirsch L, et al. Nanoshell-Enabled Photonics-Based Imaging and Therapy of Cancer. *Technol Cancer Res Treat*. 2004;3(1):33-40. doi:10.1177/153303460400300104

14. Tenchov R, Bird R, Curtze AE, Zhou Q. Lipid Nanoparticles─From Liposomes to mRNA Vaccine Delivery, a Landscape of Research Diversity and Advancement. *ACS Nano*. 2021;15(11):16982-17015. doi:10.1021/acsnano.1c04996

15. Malam Y, Loizidou M, Seifalian AM. Liposomes and nanoparticles: nanosized vehicles for drug delivery in cancer. *Trends in Pharmacological Sciences*. 2009;30(11):592-599. doi:10.1016/j.tips.2009.08.004

16. Bozzuto G, Molinari A. Liposomes as nanomedical devices. *IJN*. Published online February 2015:975. doi:10.2147/IJN.S68861

17. Palmerston Mendes L, Pan J, Torchilin V. Dendrimers as Nanocarriers for Nucleic Acid and Drug Delivery in Cancer Therapy. *Molecules*. 2017;22(9):1401. doi:10.3390/molecules22091401

18. Tomalia DA, Baker H, Dewald J, et al. A New Class of Polymers: Starburst-Dendritic Macromolecules. *Polym J*. 1985;17(1):117-132. doi:10.1295/polymj.17.117

19. Hawker CJ, Frechet JMJ. Preparation of polymers with controlled molecular architecture. A new convergent approach to dendritic macromolecules. *J Am Chem Soc*. 1990;112(21):7638-7647. doi:10.1021/ja00177a027

20. Šebestík J, Reiniš M, Ježek J. Synthesis of Dendrimers: Convergent and Divergent Approaches. In: *Biomedical Applications of Peptide-, Glyco- and Glycopeptide Dendrimers, and Analogous Dendrimeric Structures*. Springer Vienna; 2012:55-81. doi:10.1007/978-3-7091-1206-9_6

21. Rashad AM. Effect of carbon nanotubes (CNTs) on the properties of traditional cementitious materials. *Construction and Building Materials*. 2017;153:81-101. doi:10.1016/j.conbuildmat.2017.07.089

22. Yu X, Gao D, Gao L, et al. Inhibiting Metastasis and Preventing Tumor Relapse by Triggering Host Immunity with Tumor-Targeted Photodynamic Therapy Using Photosensitizer-Loaded Functional Nanographenes. *ACS Nano*. 2017;11(10):10147-10158. doi:10.1021/acsnano.7b04736

23. Miyata K, Christie RJ, Kataoka K. Polymeric micelles for nano-scale drug delivery. *Reactive and Functional Polymers*. 2011;71(3):227-234. doi:10.1016/j.reactfunctpolym.2010.10.009

24. Sung JC, Pulliam BL, Edwards DA. Nanoparticles for drug delivery to the lungs. *Trends in Biotechnology*. 2007;25(12):563-570. doi:10.1016/j.tibtech.2007.09.005

25. El-Say KM, El-Sawy HS. Polymeric nanoparticles: Promising platform for drug delivery. *International Journal of Pharmaceutics*. 2017;528(1-2):675-691. doi:10.1016/j.ijpharm.2017.06.052

26. Anton N, Benoit JP, Saulnier P. Design and production of nanoparticles formulated from nano-emulsion templates—A review. *Journal of Controlled Release*. 2008;128(3):185-199. doi:10.1016/j.jconrel.2008.02.007

27. Schacht E, Vandorpe J, Dejardin S, Lemmouchi Y, Seymour L. Biomedical applications of degradable polyphosphazenes. *Biotechnol Bioeng*. 1996;52(1):102-108. doi:10.1002/(SICI)1097-0290(19961005)52:1<102::AID-BIT10>3.0.CO;2-Q

28. Asua JM. Emulsion polymerization: From fundamental mechanisms to process developments: Highlight. *J Polym Sci A Polym Chem*. 2004;42(5):1025-1041. doi:10.1002/pola.11096

29. Thickett SC, Gilbert RG. Emulsion polymerization: State of the art in kinetics and mechanisms. *Polymer*. 2007;48(24):6965-6991. doi:10.1016/j.polymer.2007.09.031

30. Rao JP, Geckeler KE. Polymer nanoparticles: Preparation techniques and size-control parameters. *Progress in Polymer Science*. 2011;36(7):887-913. doi:10.1016/j.progpolymsci.2011.01.001

31. Yan X, Bernard J, Ganachaud F. Nanoprecipitation as a simple and straightforward process to create complex polymeric colloidal morphologies. *Advances in Colloid and Interface Science*. 2021;294:102474. doi:10.1016/j.cis.2021.102474

32. Liu Y, Yang G, Zou D, et al. Formulation of Nanoparticles Using Mixing-Induced Nanoprecipitation for Drug Delivery. *Ind Eng Chem Res*. 2020;59(9):4134-4149. doi:10.1021/acs.iecr.9b04747

33. Fang M, Peng C wei, Pang DW, Li Y. Quantum Dots for Cancer Research: Current Status, Remaining Issues, and Future Perspectives. *Cancer Biol Med*. 2012;9:151-163.

34. Pp S, V I, T S. Gold nanoshells: A ray of hope in cancer diagnosis and treatment. *Nucl Med Biomed Imaging*. 2017;2(2). doi:10.15761/NMBI.1000122

35. Yang W, Liang H, Ma S, Wang D, Huang J. Gold nanoparticle based photothermal therapy: Development and application for effective cancer treatment. *Sustainable Materials and Technologies*. 2019;22:e00109. doi:10.1016/j.susmat.2019.e00109

36. Singh P, Pandit S, Mokkapati VRSS, Garg A, Ravikumar V, Mijakovic I. Gold Nanoparticles in Diagnostics and Therapeutics for Human Cancer. *IJMS*. 2018;19(7):1979. doi:10.3390/ijms19071979

37. Julien DC, Behnke S, Wang G, Murdoch GK, Hill RA. Utilization of monoclonal antibody-targeted nanomaterials in the treatment of cancer. *mAbs*. 2011;3(5):467-478. doi:10.4161/mabs.3.5.16089

38. Chis AA, Dobrea C, Morgovan C, et al. Applications and Limitations of Dendrimers in Biomedicine. *Molecules*. 2020;25(17):3982. doi:10.3390/molecules25173982

39. Zhang Y, Li M, Gao X, Chen Y, Liu T. Nanotechnology in cancer diagnosis: progress, challenges and opportunities. *J Hematol Oncol*. 2019;12(1):137. doi:10.1186/s13045-019-0833-3

40. Schipper ML, Iyer G, Koh AL, et al. Particle Size, Surface Coating, and PEGylation Influence the Biodistribution of Quantum Dots in Living Mice. *Small*. 2009;5(1):126-134. doi:10.1002/smll.200800003

41. Guerrini L, Alvarez-Puebla R, Pazos-Perez N. Surface Modifications of Nanoparticles for Stability in Biological Fluids. *Materials*. 2018;11(7):1154. doi:10.3390/ma11071154

42. Han HS, Martin JD, Lee J, et al. Spatial Charge Configuration Regulates Nanoparticle Transport and Binding Behavior In Vivo. *Angew Chem Int Ed*. 2013;52(5):1414-1419. doi:10.1002/anie.201208331

43. Clemons TD, Singh R, Sorolla A, Chaudhari N, Hubbard A, Iyer KS. Distinction Between Active and Passive Targeting of Nanoparticles Dictate Their Overall Therapeutic Efficacy. *Langmuir*. 2018;34(50):15343-15349. doi:10.1021/acs.langmuir.8b02946

44. Golombek SK, May JN, Theek B, et al. Tumor targeting via EPR: Strategies to enhance patient responses. *Advanced Drug Delivery Reviews*. 2018;130:17-38. doi:10.1016/j.addr.2018.07.007

45. Matsumura Y, Maeda H. A New Concept for Macromolecular Therapeutics in Cancer Chemotherapy: Mechanism of Tumoritropic Accumulation of Proteins and the Antitumor Agent Smancs. :7.

46. Figueiredo P, Bauleth-Ramos T, Hirvonen J, Sarmento B, Santos HA. The Emerging Role of Multifunctional Theranostic Materials in Cancer Nanomedicine. In: *Handbook of Nanomaterials for Cancer Theranostics*. Elsevier; 2018:1-31. doi:10.1016/B978-0-12-813339-2.00001-3

47. Bertrand N, Wu J, Xu X, Kamaly N, Farokhzad OC. Cancer nanotechnology: The impact of passive and active targeting in the era of modern cancer biology. *Advanced Drug Delivery Reviews*. 2014;66:2-25. doi:10.1016/j.addr.2013.11.009

48. Pearce AK, O'Reilly RK. Insights into Active Targeting of Nanoparticles in Drug Delivery: Advances in Clinical Studies and Design Considerations for Cancer Nanomedicine. *Bioconjugate Chem*. 2019;30(9):2300-2311. doi:10.1021/acs.bioconjchem.9b00456

49. Conde J, Dias JT, GrazÃº V, Moros M, Baptista PV, de la Fuente JM. Revisiting 30 years of biofunctionalization and surface chemistry of inorganic nanoparticles for nanomedicine. *Front Chem*. 2014;2. doi:10.3389/fchem.2014.00048

50. Salahpour Anarjan F. Active targeting drug delivery nanocarriers: Ligands. *Nano-Structures & Nano-Objects*. 2019;19:100370. doi:10.1016/j.nanoso.2019.100370

51. Ruoslahti E. Peptides as Targeting Elements and Tissue Penetration Devices for Nanoparticles. *Adv Mater*. 2012;24(28):3747-3756. doi:10.1002/adma.201200454

52. Yoo J, Park C, Yi G, Lee D, Koo H. Active Targeting Strategies Using Biological Ligands for Nanoparticle Drug Delivery Systems. *Cancers*. 2019;11(5):640. doi:10.3390/cancers11050640

53. Yang Y, Chen Q, Li S, et al. iRGD-Mediated and Enzyme-Induced Precise Targeting and Retention of Gold Nanoparticles for the Enhanced Imaging and Treatment of Breast Cancer. *j biomed nanotechnol*. 2018;14(8):1396-1408. doi:10.1166/jbn.2018.2592

54. Guo Z, Peng H, Kang J, Sun D. Cell-penetrating peptides: Possible transduction mechanisms and therapeutic applications. *Biomedical Reports*. 2016;4(5):528-534. doi:10.3892/br.2016.639

55. Heitz F, Morris MC, Divita G. Twenty years of cell-penetrating peptides: from molecular mechanisms to therapeutics: Peptide-based drug delivery technology. *British Journal of Pharmacology*. 2009;157(2):195-206. doi:10.1111/j.1476-5381.2009.00057.x

56. Ruseska I, Zimmer A. Internalization mechanisms of cell-penetrating peptides. *Beilstein J Nanotechnol*. 2020;11:101-123. doi:10.3762/bjnano.11.10

57. Derakhshankhah H, Jafari S. Cell penetrating peptides: A concise review with emphasis on biomedical applications. *Biomedicine & Pharmacotherapy*. 2018;108:1090-1096. doi:10.1016/j.biopha.2018.09.097

58. Guidotti G, Brambilla L, Rossi D. Cell-Penetrating Peptides: From Basic Research to Clinics. *Trends in Pharmacological Sciences*. 2017;38(4):406-424. doi:10.1016/j.tips.2017.01.003

59. Frankel AD, Pabo CO. Cellular uptake of the tat protein from human immunodeficiency virus. *Cell*. 1988;55(6):1189-1193. doi:10.1016/0092-8674(88)90263-2

60. Silva S, Almeida A, Vale N. Combination of Cell-Penetrating Peptides with Nanoparticles for Therapeutic Application: A Review. *Biomolecules*. 2019;9(1):22. doi:10.3390/biom9010022

61. Aroui S, Kenani A. Cell-Penetrating Peptides: A Challenge for Drug Delivery. In: Stefaniu A,

Rasul A, Hussain G, eds. *Cheminformatics and Its Applications*. IntechOpen; 2020. doi:10.5772/intechopen.91684

62. Young Kim H, Young Yum S, Jang G, Ahn DR. Discovery of a non-cationic cell penetrating peptide derived from membrane-interacting human proteins and its potential as a protein delivery carrier. *Sci Rep*. 2015;5(1):11719. doi:10.1038/srep11719

63. Gao S, Simon MJ, Hue CD, Morrison B, Banta S. An Unusual Cell Penetrating Peptide Identified Using a Plasmid Display-Based Functional Selection Platform. *ACS Chem Biol*. 2011;6(5):484-491. doi:10.1021/cb100423u

64. Green M, Loewenstein PM. Autonomous functional domains of chemically synthesized human immunodeficiency virus tat trans-activator protein. *Cell*. 1988;55(6):1179-1188. doi:10.1016/0092-8674(88)90262-0

65. Derossi D, Joliot AH, Chassaing G, Prochiantz A. The third helix of the Antennapedia homeodomain translocates through biological membranes. *J Biol Chem*. 1994;269(14):10444-10450.

66. Byun Y, Singh VK, Yang VC. Low Molecular Weight Protamine. *Thrombosis Research*. 1999;94(1):53-61. doi:10.1016/S0049-3848(98)00201-1

67. Mitchell DJ, Steinman L, Kim DT, Fathman CG, Rothbard JB. Polyarginine enters cells more efficiently than other polycationic homopolymers: Cellular uptake of polyarginine. *The Journal of Peptide Research*. 2000;56(5):318-325. doi:10.1034/j.1399-3011.2000.00723.x

68. Lai JR, Huck BR, Weisblum B, Gellman SH. Design of Non-Cysteine-Containing Antimicrobial β-Hairpins: Structure−Activity Relationship Studies with Linear Protegrin-1 Analogues. *Biochemistry*. 2002;41(42):12835-12842. doi:10.1021/bi026127d

69. Anunthawan T, Yaraksa N, Phosri S, et al. Improving the antibacterial activity and selectivity of an ultra short peptide by hydrophobic and hydrophilic amino acid stretches. *Bioorganic & Medicinal Chemistry Letters*. 2013;23(16):4657-4662. doi:10.1016/j.bmcl.2013.06.005

70. Ziegler A, Nervi P, Dürrenberger M, Seelig J. The Cationic Cell-Penetrating Peptide CPP $^{TAT}$ Derived from the HIV-1 Protein TAT Is Rapidly Transported into Living Fibroblasts: Optical, Biophysical, and Metabolic Evidence. *Biochemistry*. 2005;44(1):138-148. doi:10.1021/bi0491604

71. He H, Ye J, Liu E, Liang Q, Liu Q, Yang VC. Low molecular weight protamine (LMWP): A nontoxic protamine substitute and an effective cell-penetrating peptide. *Journal of Controlled Release*. 2014;193:63-73. doi:10.1016/j.jconrel.2014.05.056

72. Jallouk AP, Palekar RU, Pan H, Schlesinger PH, Wickline SA. Modifications of Natural Peptides for Nanoparticle and Drug Design. In: *Advances in Protein Chemistry and Structural Biology*. Vol 98. Elsevier; 2015:57-91. doi:10.1016/bs.apcsb.2014.12.001

73. Allolio C, Magarkar A, Jurkiewicz P, et al. Arginine-rich cell-penetrating peptides induce membrane multilamellarity and subsequently enter via formation of a fusion pore. *Proc Natl Acad Sci USA*. 2018;115(47):11923-11928. doi:10.1073/pnas.1811520115

74. Kokryakov VN, Harwig SSL, Panyutich EA, et al. Protegrins: leukocyte antimicrobial peptides that combine features of corticostatic defensins and tachyplesins. *FEBS Letters*. 1993;327(2):231-236. doi:10.1016/0014-5793(93)80175-T

75. Soundrarajan N, Park S, Le Van Chanh Q, et al. Protegrin-1 cytotoxicity towards mammalian cells positively correlates with the magnitude of conformational changes of the unfolded form upon cell interaction. *Sci Rep*. 2019;9(1):11569. doi:10.1038/s41598-019-47955-2

76. Rousselle C, Clair P, Smirnova M, et al. Improved Brain Uptake and Pharmacological Activity of Dalargin Using a Peptide-Vector-Mediated Strategy. *J Pharmacol Exp Ther*. 2003;306(1):371-

376. doi:10.1124/jpet.102.048520

77. Maijaroen S, Jangpromma N, Daduang J, Klaynongsruang S. KT2 and RT2 modified antimicrobial peptides derived from Crocodylus siamensis Leucrocin I show activity against human colon cancer HCT-116 cells. *Environmental Toxicology and Pharmacology*. 2018;62:164-176. doi:10.1016/j.etap.2018.07.007

78. Gao C, Mao S, Ditzel HJ, et al. A cell-penetrating peptide from a novel pVII–pIX phage-displayed random peptide library. *Bioorganic & Medicinal Chemistry*. 2002;10(12):4057-4065. doi:10.1016/S0968-0896(02)00340-1

79. Lin YZ, Yao S, Veach RA, Torgerson TR, Hawiger J. Inhibition of Nuclear Translocation of Transcription Factor NF-κB by a Synthetic Peptide Containing a Cell Membrane-permeable Motif and Nuclear Localization Sequence. *Journal of Biological Chemistry*. 1995;270(24):14255-14258. doi:10.1074/jbc.270.24.14255

80. Rhee M, Davis P. Mechanism of Uptake of C105Y, a Novel Cell-penetrating Peptide. *Journal of Biological Chemistry*. 2006;281(2):1233-1240. doi:10.1074/jbc.M509813200

81. Gomez JA, Chen J, Ngo J, et al. Cell-Penetrating Penta-Peptides (CPP5s): Measurement of Cell Entry and Protein-Transduction Activity. *Pharmaceuticals*. 2010;3(12):3594-3613. doi:10.3390/ph3123594

82. Mansukhani A, Moscatelli D, Talarico D, Levytska V, Basilico C. A murine fibroblast growth factor (FGF) receptor expressed in CHO cells is activated by basic FGF and Kaposi FGF. *Proceedings of the National Academy of Sciences*. 1990;87(11):4378-4382. doi:10.1073/pnas.87.11.4378

83. Oehlke J, Scheller A, Wiesner B, et al. Cellular uptake of an α-helical amphipathic model peptide with the potential to deliver polar compounds into the cell interior non-endocytically. *Biochimica et Biophysica Acta (BBA) - Biomembranes*. 1998;1414(1-2):127-139. doi:10.1016/S0005-2736(98)00161-8

84. Deshayes S, Plénat T, Aldrian-Herrada G, Divita G, Le Grimellec C, Heitz F. Primary Amphipathic Cell-Penetrating Peptides: Structural Requirements and Interactions with Model Membranes. *Biochemistry*. 2004;43(24):7698-7706. doi:10.1021/bi049298m

85. Nan YH, Park IS, Hahm KS, Shin SY. Antimicrobial activity, bactericidal mechanism and LPS-neutralizing activity of the cell-penetrating peptide pVEC and its analogs: CELL-PENETRATING PEPTIDE pVEC AND ITS ANALOGS. *J Pept Sci*. 2011;17(12):812-817. doi:10.1002/psc.1408

86. Johansson HJ, El-Andaloussi S, Holm T, et al. Characterization of a Novel Cytotoxic Cell-penetrating Peptide Derived From p14ARF Protein. *Molecular Therapy*. 2008;16(1):115-123. doi:10.1038/sj.mt.6300346

87. Magzoub M, Sandgren S, Lundberg P, et al. N-terminal peptides from unprocessed prion proteins enter cells by macropinocytosis. *Biochemical and Biophysical Research Communications*. 2006;348(2):379-385. doi:10.1016/j.bbrc.2006.07.065

88. Oehlke J, Krause E, Wiesner B, Beyermann M, Bienert M. Extensive cellular uptake into endothelial cells of an amphipathic β-sheet forming peptide. *FEBS Letters*. 1997;415(2):196-199. doi:10.1016/S0014-5793(97)01123-X

89. Morris M. A new peptide vector for efficient delivery of oligonucleotides into mammalian cells. *Nucleic Acids Research*. 1997;25(14):2730-2736. doi:10.1093/nar/25.14.2730

90. Elmquist A, Lindgren M, Bartfai T, Langel Ü. VE-Cadherin-Derived Cell-Penetrating Peptide, pVEC, with Carrier Functions. *Experimental Cell Research*. 2001;269(2):237-244. doi:10.1006/excr.2001.5316

91. Yamada T, Mehta RR, Lekmine F, et al. A peptide fragment of azurin induces a p53-mediated cell cycle arrest in human breast cancer cells. *Mol Cancer Ther*. 2009;8(10):2947-2958. doi:10.1158/1535-7163.MCT-09-0444

92. Kondo E, Saito K, Tashiro Y, et al. Tumour lineage-homing cell-penetrating peptides as anticancer molecular delivery systems. *Nat Commun*. 2012;3(1):951. doi:10.1038/ncomms1952

93. Simeoni F. Insight into the mechanism of the peptide-based gene delivery system MPG: implications for delivery of siRNA into mammalian cells. *Nucleic Acids Research*. 2003;31(11):2717-2724. doi:10.1093/nar/gkg385

94. Crombez L, Morris MC, Dufort S, et al. Targeting cyclin B1 through peptide-based delivery of siRNA prevents tumour growth. *Nucleic Acids Research*. 2009;37(14):4559-4569. doi:10.1093/nar/gkp451

95. Akdag IO, Ozkirimli E. The Uptake Mechanism of the Cell-Penetrating pVEC Peptide. *Journal of Chemistry*. 2013;2013:1-9. doi:10.1155/2013/851915

96. Gao H, Zhang Q, Yang Y, Jiang X, He Q. Tumor homing cell penetrating peptide decorated nanoparticles used for enhancing tumor targeting delivery and therapy. *International Journal of Pharmaceutics*. 2015;478(1):240-250. doi:10.1016/j.ijpharm.2014.11.029

97. Yamada T, Goto M, Punj V, et al. Bacterial redox protein azurin, tumor suppressor protein p53, and regression of cancer. *Proceedings of the National Academy of Sciences*. 2002;99(22):14098-14103. doi:10.1073/pnas.222539699

98. Yaghoubi A, Khazaei M, Avan A, Hasanian SM, Cho WC, Soleimanpour S. p28 Bacterial Peptide, as an Anticancer Agent. *Front Oncol*. 2020;10:1303. doi:10.3389/fonc.2020.01303

99. Huang F, Shu Q, Qin Z, et al. Anticancer Actions of Azurin and Its Derived Peptide p28. *Protein J*. 2020;39(2):182-189. doi:10.1007/s10930-020-09891-3

100. Lulla RR, Goldman S, Yamada T, et al. Phase I trial of p28 (NSC745104), a non-HDM2-mediated peptide inhibitor of p53 ubiquitination in pediatric patients with recurrent or progressive central nervous system tumors: A Pediatric Brain Tumor Consortium Study. *NEUONC*. 2016;18(9):1319-1325. doi:10.1093/neuonc/now047

101. Habault J, Poyet JL. Recent Advances in Cell Penetrating Peptide-Based Anticancer Therapies. *Molecules*. 2019;24(5):927. doi:10.3390/molecules24050927

102. Khan MM, Filipczak N, Torchilin VP. Cell penetrating peptides: A versatile vector for co-delivery of drug and genes in cancer. *Journal of Controlled Release*. 2021;330:1220-1228. doi:10.1016/j.jconrel.2020.11.028

103. Tripathi PP, Arami H, Banga I, Gupta J, Gandhi S. Cell penetrating peptides in preclinical and clinical cancer diagnosis and therapy. *Oncotarget*. 2018;9(98):37252-37267. doi:10.18632/oncotarget.26442

104. Feni L, Neundorf I. The Current Role of Cell-Penetrating Peptides in Cancer Therapy. In: Sunna A, Care A, Bergquist PL, eds. *Peptides and Peptide-Based Biomaterials and Their Biomedical Applications*. Vol 1030. Advances in Experimental Medicine and Biology. Springer International Publishing; 2017:279-295. doi:10.1007/978-3-319-66095-0_13

105. Gomarasca M, F. C. Martins T, Greune L, Hardwidge PR, Schmidt MA, Rüter C. Bacterium-Derived Cell-Penetrating Peptides Deliver Gentamicin To Kill Intracellular Pathogens. *Antimicrob Agents Chemother*. 2017;61(4). doi:10.1128/AAC.02545-16

106. Galdiero S, Falanga A, Morelli G, Galdiero M. gH625: A milestone in understanding the many roles of membranotropic peptides. *Biochimica et Biophysica Acta (BBA) - Biomembranes*. 2015;1848(1):16-25. doi:10.1016/j.bbamem.2014.10.006

107. Gessner I, Neundorf I. Nanoparticles Modified with Cell-Penetrating Peptides: Conjugation Mechanisms, Physicochemical Properties, and Application in Cancer Diagnosis and Therapy. *IJMS*. 2020;21(7):2536. doi:10.3390/ijms21072536

108. Wu X, Yang H, Yang W, et al. Nanoparticle-based diagnostic and therapeutic systems for brain tumors. *J Mater Chem B*. 2019;7(31):4734-4750. doi:10.1039/C9TB00860H

109. Rong L, Qin SY, Zhang C, et al. Biomedical applications of functional peptides in nano-systems. *Materials Today Chemistry*. 2018;9:91-102. doi:10.1016/j.mtchem.2018.06.001

110. Gao H, Qian J, Cao S, et al. Precise glioma targeting of and penetration by aptamer and peptide dual-functioned nanoparticles. *Biomaterials*. 2012;33(20):5115-5123. doi:10.1016/j.biomaterials.2012.03.058

111. Kanazawa T, Akiyama F, Kakizaki S, Takashima Y, Seta Y. Delivery of siRNA to the brain using a combination of nose-to-brain delivery and cell-penetrating peptide-modified nano-micelles. *Biomaterials*. 2013;34(36):9220-9226. doi:10.1016/j.biomaterials.2013.08.036

112. Asai T, Tsuzuku T, Takahashi S, et al. Cell-penetrating peptide-conjugated lipid nanoparticles for siRNA delivery. *Biochemical and Biophysical Research Communications*. 2014;444(4):599-604. doi:10.1016/j.bbrc.2014.01.107

113. Hossain MdK, Cho HY, Kim KJ, Choi JW. In situ monitoring of doxorubicin release from biohybrid nanoparticles modified with antibody and cell-penetrating peptides in breast cancer cells using surface-enhanced Raman spectroscopy. *Biosensors and Bioelectronics*. 2015;71:300-305. doi:10.1016/j.bios.2015.04.053

114. Jin C, Bai L, Lin L, Wang S, Yin X. Paclitaxel-loaded nanoparticles decorated with bivalent fragment HAb18 F(ab')$_2$ and cell penetrating peptide for improved therapeutic effect on hepatocellular carcinoma. *Artificial Cells, Nanomedicine, and Biotechnology*. 2018;46(5):1076-1084. doi:10.1080/21691401.2017.1360325

115. Hong ST, Lin H, Wang CS, et al. Improving the anticancer effect of afatinib and microRNA by using lipid polymeric nanoparticles conjugated with dual pH-responsive and targeting peptides. *J Nanobiotechnol*. 2019;17(1):89. doi:10.1186/s12951-019-0519-6

116. Lo YL, Chang CH, Wang CS, et al. PEG-coated nanoparticles detachable in acidic microenvironments for the tumor-directed delivery of chemo- and gene therapies for head and neck cancer. *Theranostics*. 2020;10(15):6695-6714. doi:10.7150/thno.45164

117. Garizo AR, Castro F, Martins C, et al. p28-functionalized PLGA nanoparticles loaded with gefitinib reduce tumor burden and metastases formation on lung cancer. *Journal of Controlled Release*. 2021;337:329-342. doi:10.1016/j.jconrel.2021.07.035

118. Balogh J, Victor D, Asham EH, et al. Hepatocellular carcinoma: a review. *JHC*. 2016;Volume 3:41-53. doi:10.2147/JHC.S61146

119. Colagrande S, Inghilesi AL, Aburas S, Taliani GG, Nardi C, Marra F. Challenges of advanced hepatocellular carcinoma. *WJG*. 2016;22(34):7645. doi:10.3748/wjg.v22.i34.7645

120. Bernabeu E, Cagel M, Lagomarsino E, Moretton M, Chiappetta DA. Paclitaxel: What has been done and the challenges remain ahead. *International Journal of Pharmaceutics*. 2017;526(1-2):474-495. doi:10.1016/j.ijpharm.2017.05.016

121. Nair N, Kasai T, Seno M. Bacteria: Prospective Savior in Battle against Cancer. *Anticancer Research*. 2014:6289-6296.

122. Paukner S, Kohl G, Lubitz W. Bacterial ghosts as novel advanced drug delivery systems: antiproliferative activity of loaded doxorubicin in human Caco-2 cells. *Journal of Controlled Release*. 2004;94(1):63-74. doi:10.1016/j.jconrel.2003.09.010

123. Yamada T, Christov K, Shilkaitis A, et al. p28, A first in class peptide inhibitor of cop1 binding to p53. *Br J Cancer*. 2013;108(12):2495-2504. doi:10.1038/bjc.2013.266

124. Yamada T, Fialho AM, Punj V, Bratescu L, Gupta TKD, Chakrabarty AM. Internalization of bacterial redox protein azurin in mammalian cells: entry domain and specificity: Entry domain of azurin. *Cellular Microbiology*. 2005;7(10):1418-1431. doi:10.1111/j.1462-5822.2005.00567.x

125. Sato AK, Viswanathan M, Kent RB, Wood CR. Therapeutic peptides: technological advances driving peptides into development. *Current Opinion in Biotechnology*. 2006;17(6):638-642. doi:10.1016/j.copbio.2006.10.002

126. Owen DM, Rentero C, Magenau A, Abu-Siniyeh A, Gaus K. Quantitative imaging of membrane lipid order in cells and organisms. *Nat Protoc*. 2012;7(1):24-35. doi:10.1038/nprot.2011.419

127. Clogston JD, Patri AK. Zeta Potential Measurement. In: McNeil SE, ed. *Characterization of Nanoparticles Intended for Drug Delivery*. Vol 697. Methods in Molecular Biology. Humana Press; 2011:63-70. doi:10.1007/978-1-60327-198-1_6

128. Danaei M, Dehghankhold M, Ataei S, et al. Impact of Particle Size and Polydispersity Index on the Clinical Applications of Lipidic Nanocarrier Systems. *Pharmaceutics*. 2018;10(2):57. doi:10.3390/pharmaceutics10020057

129. Bernardes N, Garizo AR, Pinto SN, et al. Azurin interaction with the lipid raft components ganglioside GM-1 and caveolin-1 increases membrane fluidity and sensitivity to anti-cancer drugs. *Cell Cycle*. 2018;17(13):1649-1666. doi:10.1080/15384101.2018.1489178

130. Bernardes N, Fialho A. Perturbing the Dynamics and Organization of Cell Membrane Components: A New Paradigm for Cancer-Targeted Therapies. *IJMS*. 2018;19(12):3871. doi:10.3390/ijms19123871

131. Ding X, Zhang W, Li S, Yang H. The role of cholesterol metabolism in cancer. *Am J Cancer Res.* February 1, 2019:219-227.

132. Lakowicz JR, ed. *Principles of Fluorescence Spectroscopy*. Springer US; 2006. doi:10.1007/978-0-387-46312-4

133. Gaus K, Zech T, Harder T. Visualizing membrane microdomains by Laurdan 2-photon microscopy (Review). *Molecular Membrane Biology*. 2006;23(1):41-48. doi:10.1080/09687860500466857

134. Nishida K, Nishimura S nosuke, Tanaka M. Selective Accumulation to Tumor Cells with Coacervate Droplets Formed from a Water-Insoluble Acrylate Polymer. *Biomacromolecules*. 2022;23(4):1569-1580. doi:10.1021/acs.biomac.1c01343

135. Pokorna S, Ventura AE, Santos TCB, et al. Laurdan in live cell imaging: Effect of acquisition settings, cell culture conditions and data analysis on generalized polarization measurements. *Journal of Photochemistry and Photobiology B: Biology*. 2022;228:112404. doi:10.1016/j.jphotobiol.2022.112404

136. Duchardt F, Fotin-Mleczek M, Schwarz H, Fischer R, Brock R. A Comprehensive Model for the Cellular Uptake of Cationic Cell-penetrating Peptides. *Traffic*. 2007;8(7):848-866. doi:10.1111/j.1600-0854.2007.00572.x